1661-8726/07/030383-23
DOI 10.1007/s00015-007-1238-9
Birkhäuser Verlag, Basel, 2007

Swiss j. geosci. 100 (2007) 383–405

Possible environmental effects on the evolution of the Alps-Molasse Basin system

FRITZ SCHLUNEGGER, DIRK RIEKE-ZAPP & KARL RAMSEYER

Key words: Swiss Molasse, Alps, geodynamics, climate and tectonics

ABSTRACT

We propose three partly unrelated stages in the geodynamic evolution of the Alps and the sedimentary response of the Molasse Basin. The first stage comprises the time interval between ca. 35 and 20 Ma and is characterized by a high ratio between rates of crustal accretion and surface erosion. The response of the Molasse Basin was a change from the stage of basin underfill (UMM) to overfill (USM). Because the response time of erosional processes to crustal accretion and surface uplift lasts several millions of years, the orogen first experienced a net growth until the end of the Oligocene. As a result, the Molasse basin subsided at high rates causing the topographic axis to shift to the proximal basin border and alluvial fans to establish at the thrust front. During the Aquitanian, however, ongoing erosion and downcutting in the hinterland caused sediment discharge to the basin to increase and the ratio between the rates of crustal accretion and surface erosion to decrease. The result was a progradation of the dispersal systems, and a shift of the topographic axis towards the distal basin border. The second stage started at ca. 20 Ma at a time when palaeoclimate became more continental, and when the crystalline core became exposed in the orogen. The effect was a decrease in the erosional efficiency of the Swiss Alps and hence a reduction of sediment discharge to the Molasse Basin. We propose that this decrease in sediment flux caused the Burdigalian transgression of the OMM. We also speculate that this reduction of surface erosion initiated the modification of Alpine deformation from vertically- to mainly horizontally directed extrusion (deformation of the Southern Alps, and the Jura Mountains some Ma later). The third stage in the geodynamic development was initiated at the Miocene/Pliocene boundary. At that time, palaeoclimate possibly became wetter, which, in turn, caused surface erosion to increase relative to crustal accretion. This change caused the Alps to enter a destructive stage and the locus of active deformation to shift towards to the orogenic core. It also resulted in a net unloading of the orogen and thus in a flexural rebound of the foreland plate.

We conclude that the present chronological resolution is sufficient to propose possible feedback mechanisms between environmental effects and lithospheric processes. Further progress will result from a down-scaling in research. Specifically, we anticipate that climate-driven changes in sediment flux altered the channel geometries of USM and OSM deposits, the pattern of sediment transport and thus the stacking arrangement of architectural elements. This issue has not been sufficiently explored and awaits further detailed quantitative studies.

Introduction

High-resolution chronologies of foreland basin deposits are prerequisites for relating geodynamic processes in orogens to the stratigraphic response in adjacent sedimentary troughs. This has been illustrated by detailed studies from different basins in the world (e.g., Jordan et al., 2001; Horton & DeCelles, 2001; Chen et al., 2002; von Rotz et al., 2005). This is also the case for the Oligo-Miocene evolution of the Swiss Molasse Basin located north of the Central Alps (Fig. 1). For this foreland basin, high-resolution magnetostratigraphy in combination with mammal biostratigraphy (Schlunegger et al., 1996; Kempf et al., 1999; Strunck & Matter, 2002) resulted in the establishment of a high-resolution chronological framework for the Molasse deposits (Fig. 2). These chronologies then build the basis for assignments of ages to depositional systems, dispersion directions, petrofacies and the fossiliferous record of plants (see Kuhlemann & Kempf, 2002, and Berger et al., 2005a, b; for the most recent compilations). In addition, they provide indispensable information for relating sedimentary processes to Alpine tectonic events, climate variabilites, and modifications in exposed bedrock in the Alps (e.g., Schlunegger et al., 1998; Schlunegger, 1999; Kuhlemann & Kempf, 2002). Compilations of stratigraphic data resulted in the now generally accepted knowledge that the width and the tilt direction of the basin, the pattern of subsidence rates and the location of the topographic axis are controlled by the relative importance of lithospheric processes leading to crustal thickening and loading in the Alps, and surface processes resulting in redistribution of mass from the Alps to the Molasse Basin (Pfiffner et al., 2002). Recent applications of new theoretical concepts, however, resulted in the notion that variations in erosion rates modulated the crustal velocity field in the Alps

Exogene Geology Group, Institute of Geological Sciences, University of Bern, Baltzerstrasse 1+3, 3012 Bern, Switzerland, schlunegger@geo.unibe.ch

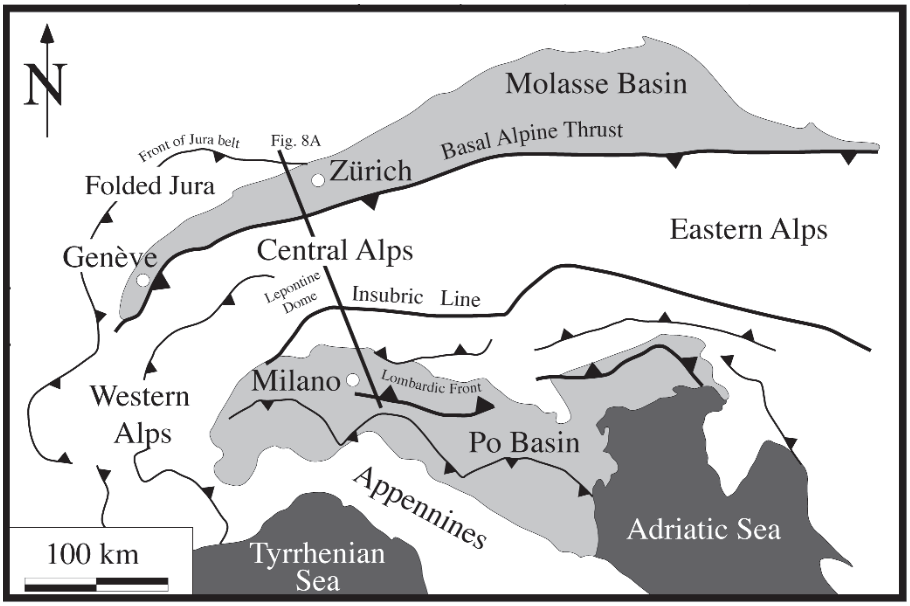

Fig. 1. Tectonic map of the Alps and adjacent foreland basins and location of tectonic cross-section

(Schlunegger & Simpson, 2002; Cederbom et al., 2004; Willett et al., 2006), and the pattern and rates of Alpine exhumation (Schlunegger & Willett, 1999).

This paper synthesizes our current understanding of how the development of the Swiss Molasse and the Central Alps chronicles possible feedback mechanisms between lithospheric thickening and sediment transfer. Three objectives related to this topic will be presented here, and their effects on the Molasse stratigraphy and the Alpine geodynamics be discussed. The first addresses the exploration of how sediment transfer from the Alps to the Molasse has driven the stratigraphic development of the foreland trough. The second and third objectives concern the interaction between sediment transfer and the crustal velocity field in the Alps thereby recognizing that (i) lithospheric deformation exerts the first order control on topography and erosion, but that (ii) (re)distribution of topographic mass potentially results in a modulation of the lithospheric stress field (Willett et al., 1993). Specifically, it is possible that the Central Alps and the Molasse Basin evolved in response to changes in the relative importance of crustal accretion and surface erosion. This is the issue that we intend to discuss in this paper. We will then conclude that the Oligocene history of the Central Alps and the Molasse was to a first order driven by tectonic processes, but that the Neogene evolutionary stages could have been modulated to substantial extents by environmental effects (such as climate-driven variations in surface erosion rates).

According to the scope, we first introduce the stratigraphy of the Swiss Molasse and summarize the development of facies and depositional systems. We then present the litho-tectonic architecture of the Central Alps together with a general view of the geodynamic evolution of this orogen. This will be followed by a presentation of data about sediment discharge and palaeoclimate. Finally, we combine these information into a synthesis thereby discussing possible effects of feedback mechanisms between lithospheric and surface processes on the evolution of the Central Alps and the Molasse.

We want to emphasize here that this synthesis is by far not complete. It is simply not possible to give insight into the wealth of available knowledge for the Swiss Molasse and the Central Alps within one single paper. For further, more detailed information the reader is referred to the many PhD and diploma theses written at the universities of Fribourg, Bern, Basel, Genève and the ETH Zürich. Also it is important to note here that this work has a strong bias as it explicitly explores possible controls of surface erosion on the development of the Alps and the Molasse.

The development of the Molasse Basin

The Molasse deposits (Figs. 2, 3) comprise four lithostratigraphic groups, for which the conventional German abbreviations are used in this paper (Matter et al., 1980). They form two coarsening-, thickening and shallowing-upward megasequences, each of them recording transitions from basin underfill to overfill (Sinclair et al., 1991; Sinclair & Allen, 1992). The first megasequence starts with the Rupelian Lower Marine Molasse unit (UMM; Untere Meeresmolasse) (Diem, 1986). These deposits are overlain by the Chattian to Aquitanian fluvio-lacustrine deposits of the Lower Freshwater Molasse (USM; Untere Süsswassermolasse) (Strunck & Matter, 2002). The second megasequence, starting with the Burdigalian transgression on a presumably truncated surface (Sinclair et al., 1991), comprises the shallow marine deposits of the Upper Marine Molasse (OMM; Obere Meeresmolasse) that interfinger with the Napf and Hörnli fan deltas at the thrust front

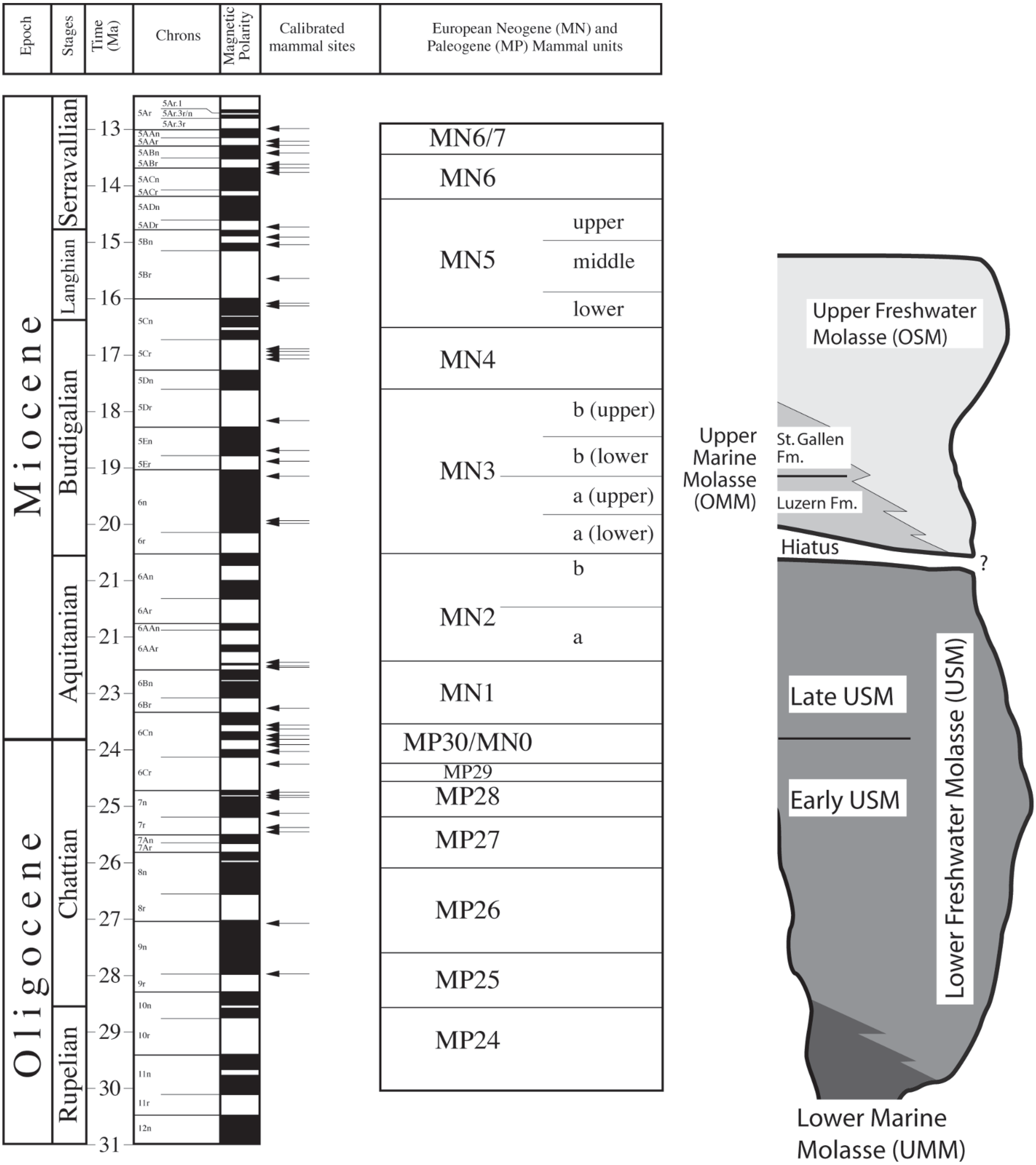

Fig. 2. Chronological framework for the lithostratigraphic groups of the Swiss Molasse Basin. It is based on the magnetostratigraphic calibration of mammal biozones. Arrows indicate mammal sites for which precise biostratigraphic and magnetostratigraphic ages are available. The lithostratigraphy is presented according to the general coarseness of the deposits (i.e. the farther right the boundary of the lithostratigraphy figure, the coarser the deposits). Note that the boundaries between Molassse units is strongly heterochronous. This supports the interpretations that changes from marine to terrestrial conditions were controlled by changes in sediment discharge. For the magnetostratigraphic data please refer to Burbank et al. (1992), Schlunegger et al. (1996), Kempf et al. (1997) and Strunck & Matter (2002). (Modified after Strunck, 2001). See Engesser (1990) for overview of biostratigraphic scheme.

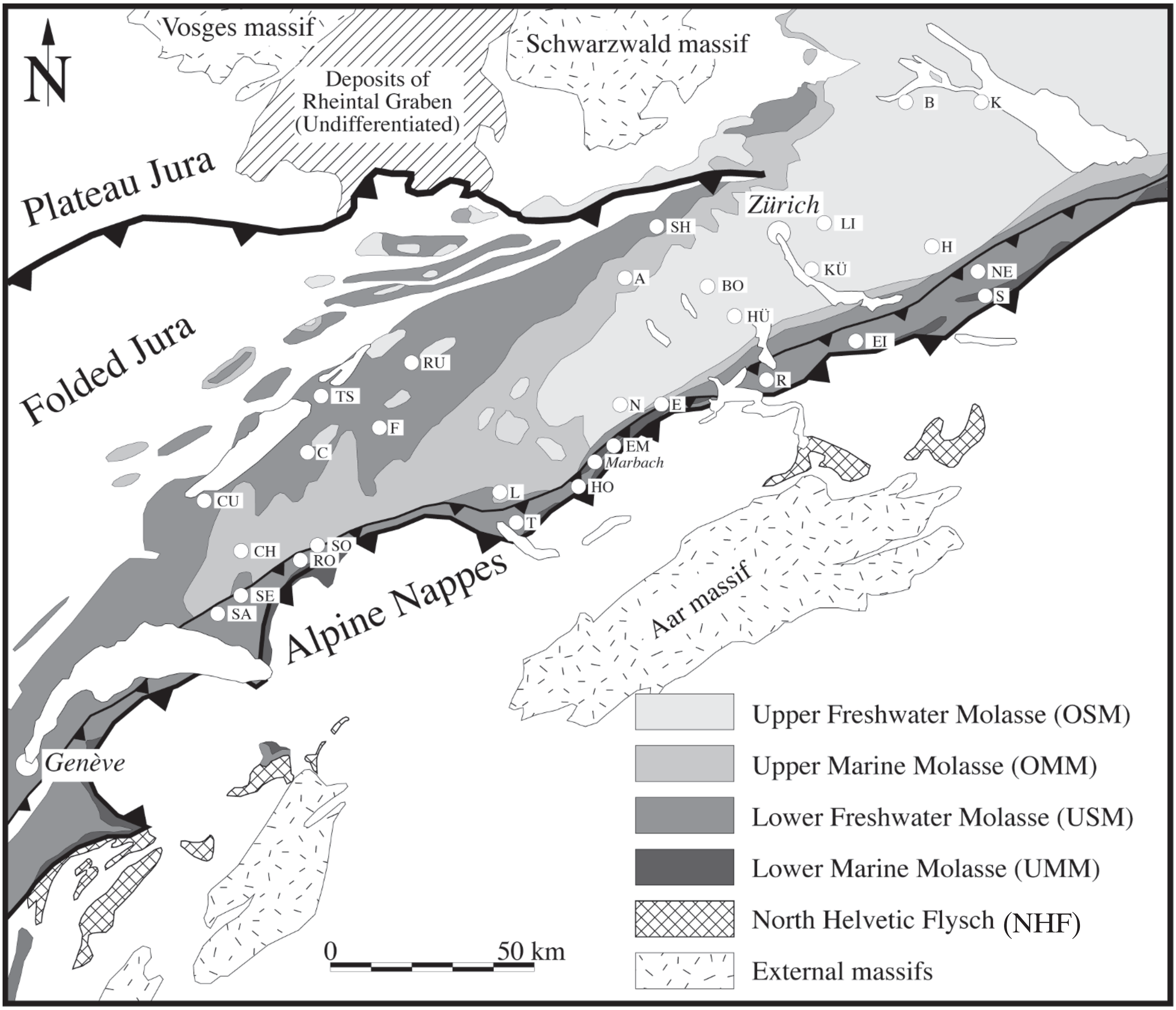

Fig. 3. Map of the Swiss Molasse Basin and locations of sections and wells (Modified after Keller et al., 1990). The thicknesses of the deposits at these sites are used to construct Figures 5 and 6. A: Altishofen-1, B: Berlingen-1, BO: Boswil-1, C: Courtion-1, CH: Chappelle-1, CU: Cuarny-1, E: Entlebuch-1, EI: Einsiedeln, EM: Emme, F: Fendringen-1, H: Hörnli, HO: Honegg, HÜ: Hünenberg-1, K: Kreuzlingen-1, KÜ: Küsnacht-1, L: Linden-1, LI: Lindau-1, N: Napf, NE: Necker, R: Rigi, RO: Romanens-1, RU: Ruppoldsried-1, S: Steintal, SA: Savigni-1, SE: Servion-1, SH: Schafisheim, SO: Sorens-1, T: Thun-1, TS: Tschugg-1. Note that selection of wells is based on the completeness of the stratigraphic section for the time spans shown in Figures 5 and 6.

(Keller, 1989). This megasequence ends with Langhian fluvial clastics of the Upper Freshwater Molasse group (OSM; Obere Süsswassermolasse). New thermo-chronometric data established at deep wells in the central part of the basin indicate that sediment accumulation of the OSM continued until the Miocene, after which the basin became inverted and exhumed (Cederbom et al., 2004; Mazurek et al., 2006). Note that some researchers consider the Lutetian to Priabonian North Helveltic Flysch (NHF) (Kempf & Pfiffner, 2004) as the first of five lithostratigraphic groups (Sinclair et al., 1991).

Lower Marine Molasse

The most classical section of middle to upper UMM is exposed at Marbach ca. 70 km southwest of Zürich (Figs. 3, 4A) (Diem, 1986). There, the UMM starts with massive to parallel-laminated marls that are interbedded with cm-thick T_{cde}- and T_{de}- turbidites (middle UMM of Diem, 1986; unit A on Fig. 4). These deposits were assigned to an offshore environment beneath the storm weather wave base (Diem, 1986). The marls are overlain by an alternation of dm-thick sandstone

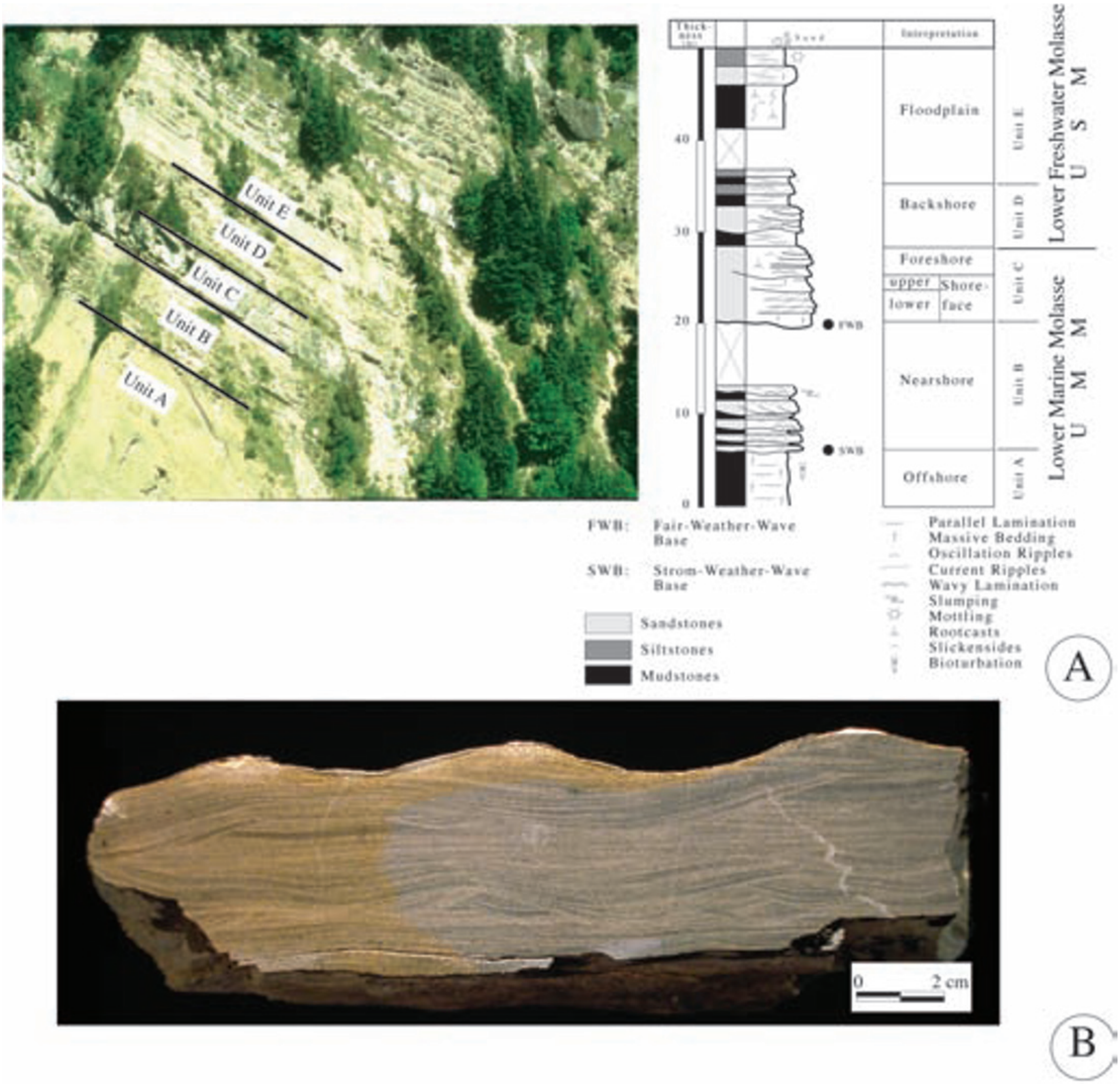

Fig. 4. (A) Sedimentological log of the Marbach section, and (B) example of a tempestite. For location of section see Figure 3.

beds and cm-thick mudstone interbeds (unit B on Fig. 4). The sandstones are normally graded and display hummocky-cross-stratifications at the base and trochoidal wave ripple cross-beds at the top (Fig. 4B). In addition, they show synsedimentary softrock deformation such as slumps and ball-and-pillow structures. The sandstone beds are considered to have been deposited by waning storms in a nearshore environment (Diem, 1986). This succession with tempestites is then overlain by a 10–20 m thick unit made up of massive and parallel-laminated sandstone beds that were presumably deposited in wave-dominated foreshore to shoreface environment (upper UMM of Diem, 1986; unit C on Fig. 4). The succeeding deposits are dm- to m-thick marls with coal and sandstone interbeds (unit D), and a succession of mottled marls with yellow to brown and red colors (Unit E; Fig. 4). These latter units are assigned to terrestrial environments and from the basis of the Lower Freshwater Molasse group (USM) (Diem, 1986).

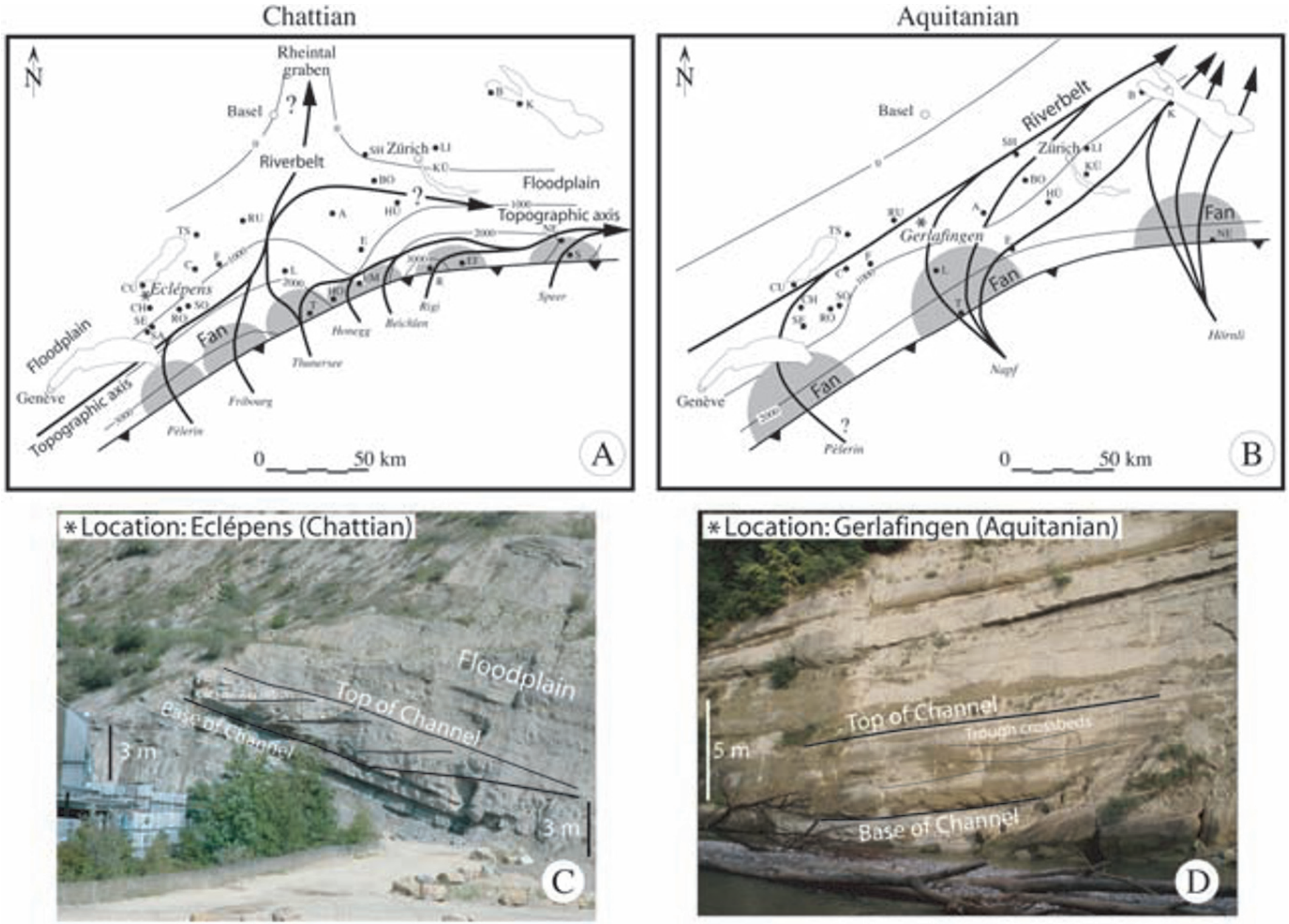

Fig. 5. Palaeogeography of USM during (A) the Chattian, and (B) the Aquitanian, and isolines of accumulated sediment thicknesses during these time intervals. (C) and (D) represent examples from the field. For compilation of thicknesses of USM and OMM strata (Fig. 6) please refer to Pfiffner et al. (2002) for eastern Molasse, and Strunck (2001) for western Molasse. For abbreviations see text of Figure 3. The thicknesses of stratigraphic sections are presented in Tab. 1.

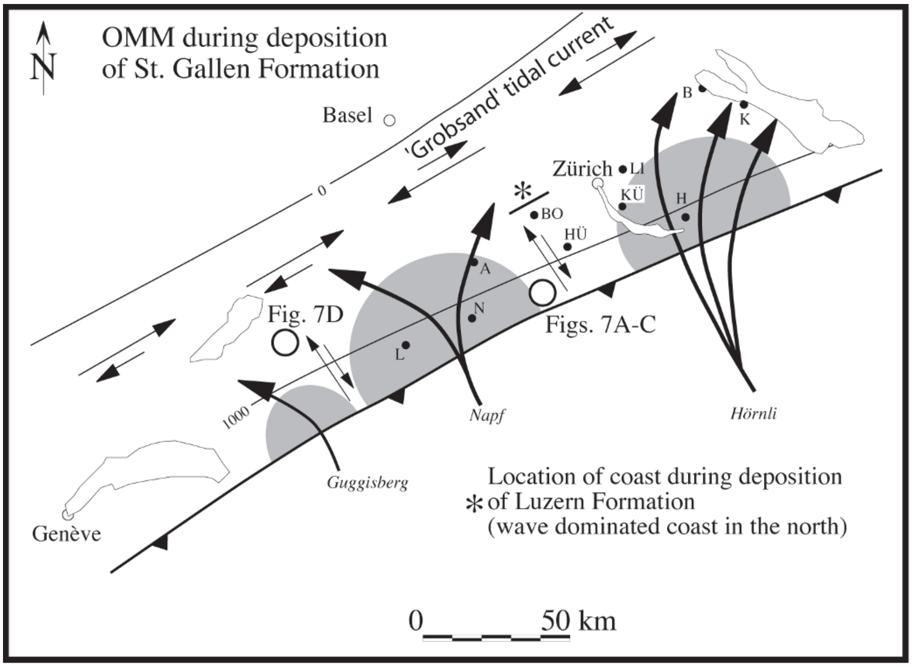

Fig. 6. Palaeogeography of OMM during deposition of the St. Gallen Fm. and isolines of accumulated thicknesses of marine deposits. Note that during the early stage of the OMM (i.e. during deposition of the Luzern Fm., Fig. 2), the width of the perialpine sea was significantly shorter (location of northern coast indicated by star southwest of Zürich). See Figure 5 for legend of wells and sections, and Allen et al. (1985) for further information. Figure 2 illustrates the stratigraphic and chronologic position of the St. Gallen and the Luzern Formations. For abbreviations see text of Figure 3. The thicknesses are of stratigraphic sections are presented in Tab. 1. Thin arrows indicate tidal currents.

Estimates of palaeowave climate and water depth from wave ripple marks at the top of the tempestites (Fig. 4B) suggest that the UMM basin widened towards the ENE, and that the UMM regression was the result of depositional processes and not of an eustatic sea-level drop (Diem, 1985). This interpretation is consistent with the heterochroneity of UMM regression between 32 and 30 Ma that possibly occurred in response to an increase in sediment discharge (Kempf & Pross, 2005; Kempf, 2006). Also, the continuous vertical succession from offshore to shoreface environments without evidence of truncation indicates a high rate of sediment aggradation in a rapidly subsiding basin.

Lower Freshwater Molasse

The Lower Freshwater Molasse (USM), deposited between ca. 30 and 20 Ma according to magneto-polarity stratigraphies (Strunck & Matter, 2002, and references therein), is made up of alluvial fan conglomerates at the thrust front with a NW-directed transverse dispersion (fans on Figs. 5A, 5B), and an NE-oriented axial drainage with sandstone riverbelts that were deposited in the topographic axis (Figs. 5A, 5B). The USM unit has a preserved thickness of >3000 m at the proximal basin border and thins to <100 m near the distal edge of the basin. Detailed sedimentological analysis of well-exposed sections reveal that the deposits of the axial drainage are made up of distinct architectural elements. Each are assigned to a particular depositional setting including riverbelts, levees, crevasse channels and splays, floodplain fines and palaeosoils, and lacustrine (Platt & Keller, 1992). The riverbelt sandstones are between 150 and 1500 m wide and arranged as amalgamated and locally stacked ribbon bodies 2–15 m thick. They comprise rip-up clasts at the base, and display epsilon- and trough-crossbeds suggesting deposition in meandering (Fig. 5C) and braided channels with a dominant bedload component (Fig. 5D). Interbedded finer-grained units are dm- to m-thick and display structures that are indicative of episodic sediment transport in the upper flow regime (massive bedding and parallel lamination in sandstones: crevasse splays and channels), or that suggest episodic deposition of suspended loads (climbing ripples, parallel lamination in mudstones, mottling: levee and floodplain deposits).

Arrangements of the transverse and axial systems are different in the Chattian and the Aquitanian. During the Chattian (Fig. 5A), approximately 7 dispersal systems discharged into the Molasse trough. They changed the dispersion direction from a transverse to an axial orientation within less than 2 km distance upon entrance into the basin (Schlunegger et al., 1997a). Note that it is unclear whether the western system was re-directed towards the Rheintal graben at that time (Kuhlemann & Kempf, 2002; Berger et al., 2005a, b; Fig. 5A). Between the Chattian and the Aquitanian, the fans prograded towards more distal sites, causing the basin axis to shift ca. 50 km farther north (Fig. 5B). This progradational trend reflects an increase in the relative importance of sediment discharge versus formation rates of accommodation space (Schlunegger et al., 1997a). In addition, the dispersal systems coalesced from approximately 7 to 3 major systems between the Chattian and the Aquitanian (Fig. 5B).

Upper Marine Molasse

Similar to the USM, the thickness of the Upper Marine Molasse group (OMM) thins from ca. 1000 m at the proximal bor-

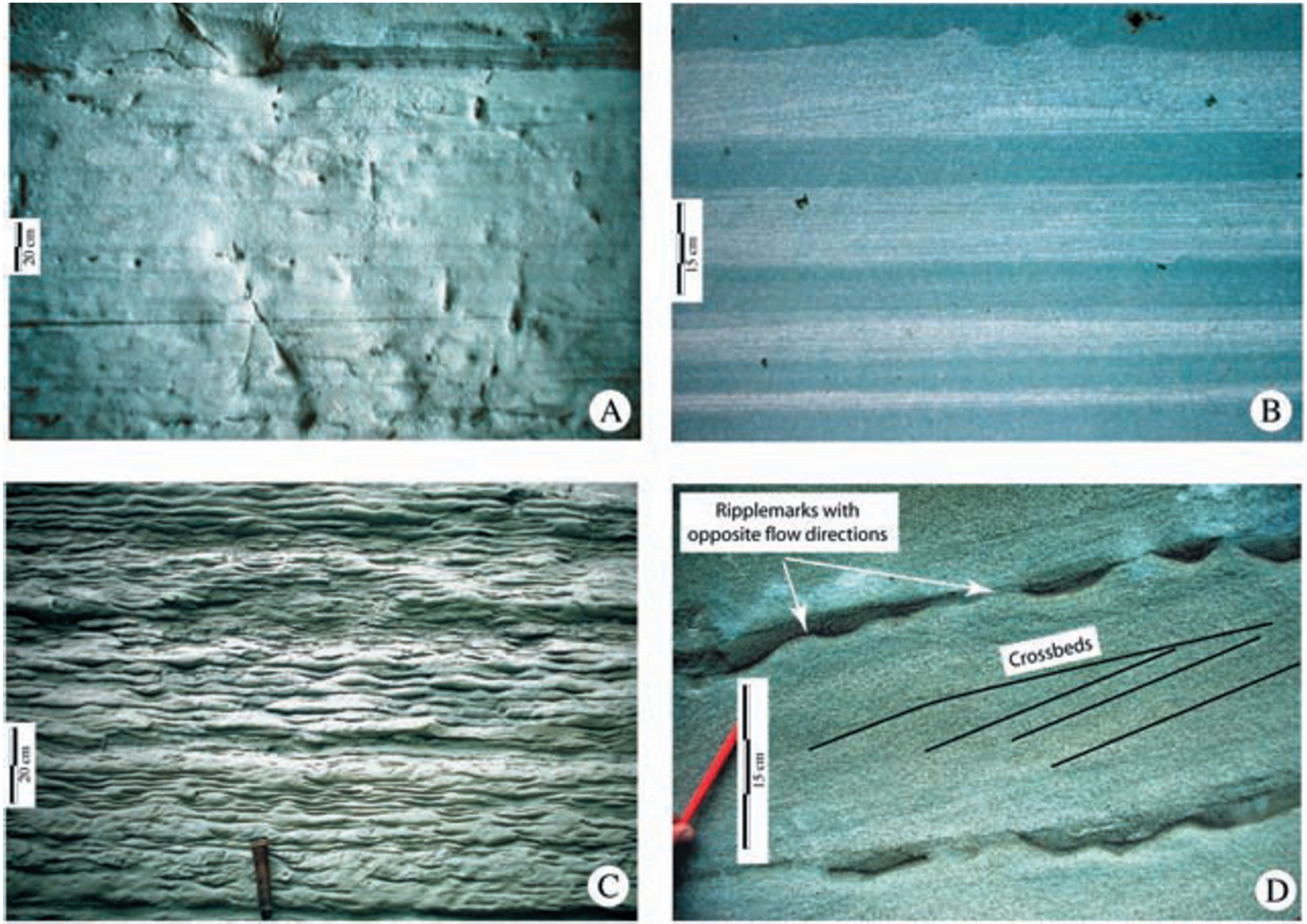

Fig. 7. Examples from OMM, showing (A) parallel laminated sandstones of proximal shoreface of Luzern Fm., (B) packages of parallel laminated sandstones with normal grading of wave breaking zone, proximal shoreface of Luzern Fm., (C) flaser bedding of sandy tidal flat of St. Gallen Fm., and (D) cross-bedded sandstones presumably deposited in a tidal channel of St. Gallen Fm. Photographs A, B and C were taken from a section 30 km south of Zürich, photograph D illustrates the OMM at a location ca. 100 km northeast of Geneva. See Figure 2 for stratigraphic and chronologic position of the St. Gallen and the Luzern Formations, and Figure 6 for location of photographs.

Table 1. Stratigraphic data of the Molasse Basin. A compilation and discussion of the data in terms of temporal resolution is presented by Schlunegger (1999). Additional data is taken from Kempf et al. (1999) for the Hörnli, Necker and Steintal sections, and from Kempf & Matter (1999) for the Zürich section, and Strunck (2001) for the sections of western Switzerland. See Figure 3 for location of sections.

well/section	compacted thicknesses (m)		
	Early USM 30–25 Ma	Late USM 25–20 Ma	OMM 20–17.5 Ma
A: Althishofen-1	120	800	>300
B: Berlingen-1	0	700	200
BO: Boswil-1	350	720	460
C: Courtion-1	700	>600	–
CH: Chappelle-1	600	800	>50
CU: Cuarny-1	300	>150	–
E: Entlebuch-1	500	2100	–
EI: Einsiedeln	2700	–	–
EM: Emme	1200	–	–
F: Fendringen-1	900	>900	–
H: Hörnli	–	–	1000
HO: Honegg	1500	–	–
HÜ: Hünenberg-1	450	1140	990
K: Kreuzlingen-1	0	1000	200
KÜ: Künsnacht-1	0	1500	550
L: Linden-1	1600	1600	1000
LI: Lindau-1	0	1050	300
N: Napf	–	–	1050
NE: Necker	1950	2050	–
R: Rigi	3600	–	–
RO: Romanens-1	1800	700	>400
RU: Ruppoldsried-1	400	>500	–
S: Steintal	1700	–	–
SA: Savigni-1	1050	>200	–
SE: Servion-1	250	1000	>100
SH: Schafisheim	0	>250	–
SO: Sorens-1	1700	900	>50
T: Thun-1	2150	1950	–
TS: Tschugg-1	250	>250	–

der to 70-100 m near the northern edge of the basin (Berger, 1983; Allen et al., 1985; Keller, 1989) (Fig. 6). Deposition of the OMM started at ca. 20 Ma (Fig. 2) after a transgression that successively progressed along the basin axis from the southwest and northeast, linking the Tethys with the Pannonian Basin (Paratethys) by a narrow seaway (Allen et al., 1985). The OMM transgression was also associated by a northward expansion of the distal margin, causing the seaway to widen from originally <50 to ca. 100 kilometres (Fig. 6) (Allen, 1984; Allen et al., 1985; Schlunegger et al., 1997b). This widening resulted in a change from the predominance of wave and microtidal (Luzern Formation) to mestotidal conditions (St. Gallen Formation, Fig. 2) (Keller, 1989). Tidal simulations (Martel et al., 1994; Bieg, 2005) implied that the tides penetrated from both the west (the Mediterranean) and the east (either the eastern Mediterranean or the Indo-Pacific Ocean).

Continuous discharge of Alpine detritus resulted in the construction of fan deltas at the proximal basin border (e.g., Napf and Hörnli). Their presence were interpreted by Allen et al. (1985) to have caused the tides to operate in two distinct cells which acted as essentially closed systems for sediment transport. This was interpreted based on the pattern of heavy minerals in the sandstone beds and on palaeocurrent data of offshore tidal sandwaves.

Continuously exposed sections of the wave and microtidal deposits of the Luzern Formation (Fig. 2) are found west of Luzern. Examples of OMM facies are parallel-laminated sandstone beds several cm thick (Fig. 7A), and 2 to 5 cm-thick packages of fining-upward sandstone beds that are massive-bedded and parallel-laminated (Fig. 7B). These units indicate deposition in the surf and wave-breaking zones, respectively. Excellent outcrops of the mesotidal deposits of the St. Gallen Formation (Fig. 2) are found near Fribourg along the Sarine river, and in the region west of Luzern. They expose sandstones with lenticular and flaser beds (Fig. 7C), and m-thick sandstone units with tabular crossbeds (Fig. 7D). These latter units also exhibit mm-thin mudstone interbeds and ripple marks with opposite flow directions between the individual sandstone foresets. These facies associations have been assigned to sand- and mudflat environments of a tidal flat, and to sandwaves in ebb-domianted tidal channels (Keller, 1989).

Upper Freshwater Molasse

Ongoing progradation of the fan deltas during OMM times resulted in basin overfill at ca. 17 Ma and the subsequent deposition of the OSM group. Similar to the situation of the USM, the OSM is characterized by km-thick coarse-grained alluvial-fan conglomerates at the proximal basin border (Napf, Hörnli and presumably Guggisberg fans). They interfinger with river-belt sandstones that were part of the west-directed axial drainage system in distal positions (Graupensandrinne).

Age assignments for the termination of OSM deposition are thwarted because of postdepositional erosion (Fig. 3). However, estimates of the depths of the partial annealing zone for apatite fission tracks at the end of OSM deposition, and determinations of apatite fission track ages beneath this zone imply that the Swiss Molasse basin most likely became inverted in the Pliocene, and that the amount of postdepositional erosion is ca. 1500 m in the central part of the basin, and >3000 m in thrusted Molasse (Cederbom et al., 2004).

Geodynamic evolution

In summary, the two progradational megasequences in the Swiss Molasse (UMM-USM, and OMM-OSM) record two periods during which sediment discharge into the basin increased more rapidly than accommodation space in the basin was formed. The result are shifts of the basin axis from the proximal basin border towards the distal margin (Fig. 5). It was only towards the end of the USM and during the early stages of the OMM when the sediment flux to the basin did not catch up with the rate at which accommodation space was formed. In addition, the data of accumulated thicknesses of Molasse deposits reveals a change in the pattern of subsidence rates espe-

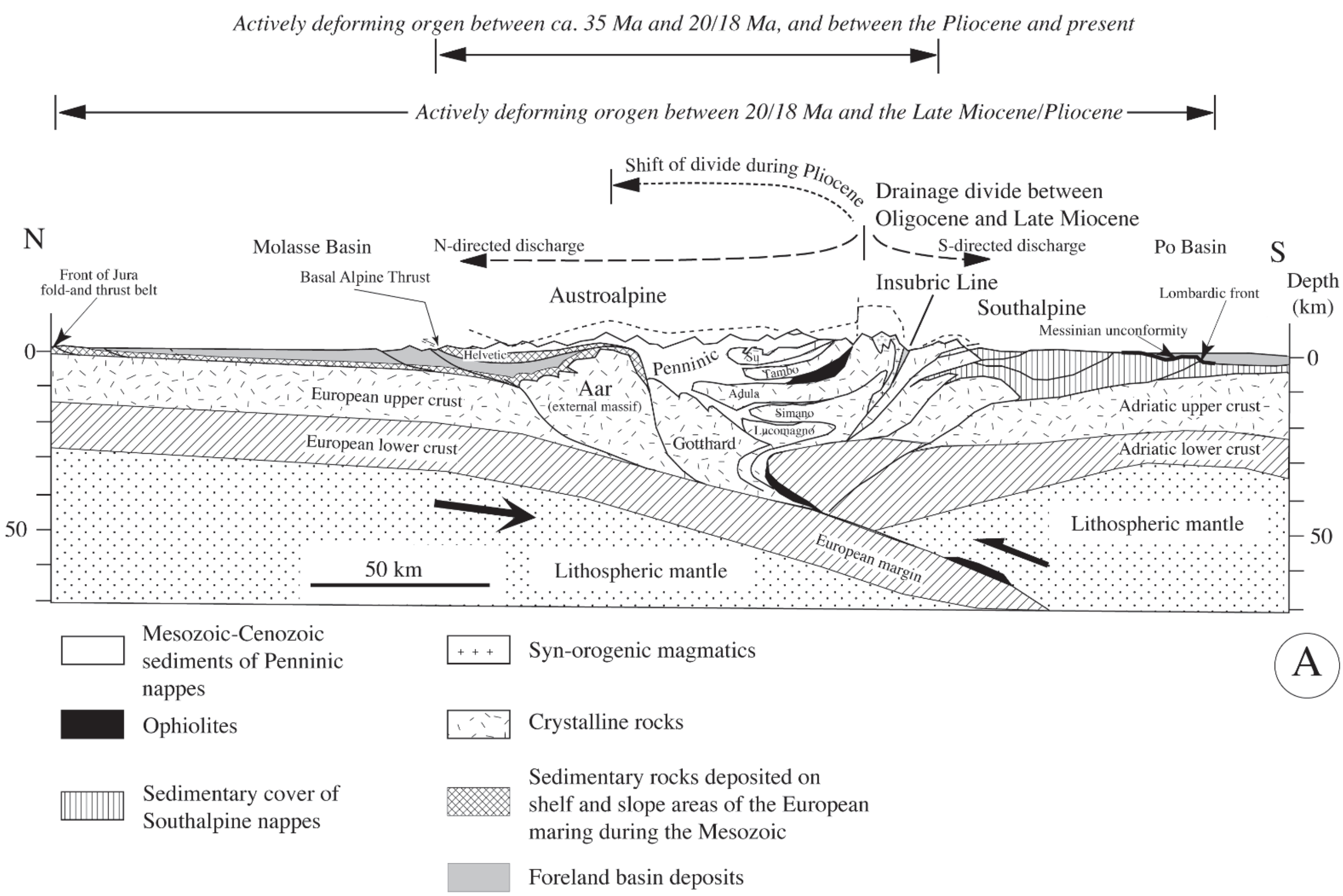

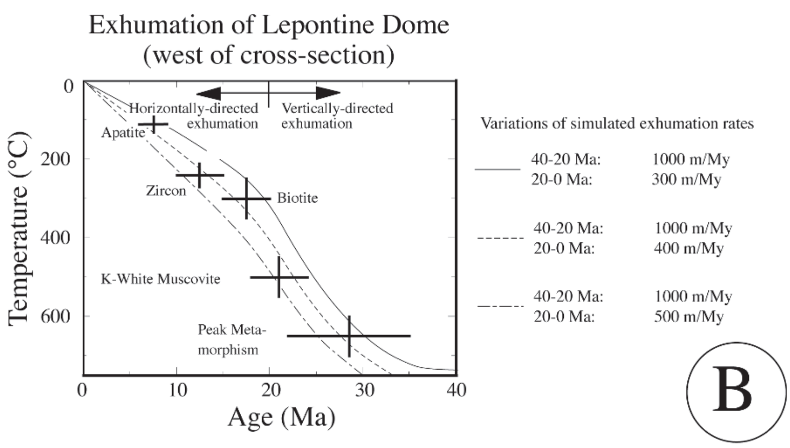

Fig. 8. Tectonic cross-section of Alps (A) after Schmid et al. (1996), and exhumation of the Lepontine (B) after Schlunegger & Willett (1999). See Figure 1 for location of cross-section. Note that the Permo-Carboniferous troughs beneath the Molasse Basin are not indicated on the cross-section.

cially between the Chattian and the Aquitanian. Specifically, the Chattian times were characterized by enhanced subsidence rates of >0.5–0.6 mm/yr (Schlunegger et al., 1997a) at the thrust front, and by the formation of a <50 km-wide basin. Also during this time span, the topographic axis was located at the proximal basin border. This situation changed in the Aquitanian. Maximum subsidence rates decreased to <0.5 mm/yr, the topographic axis shifted towards the distal basin border, and the width of the basin increased to approximately 100 km. Furthermore, the tilt direction of the basin axis was oriented towards the northeast during UMM and USM times. It then changed to the southwest thereafter. A further remarkable change in the geodynamic evolution occurred in the Pliocene when the basin became inverted and eroded (see above).

The Swiss Alps

Litho-tectonic architecture

The Swiss Alps (Fig. 8) are made up of a nappe stack that have traditionally been grouped according to the paleogeographic position during the Mesozoic phase of tectonic spreading and crustal extension. The Helvetic nappes represent the former shelf and slope areas of the European margin. They comprise a succession of alternated marls, limestones, siliceous limestones and sandstones. The rocks of the Penninic nappes are remnants that were formed in three domains: (1) the Valais trough, a basin that formed in the distal stretched part of the European margin adjacent to the Helvetic domain where mainly fine-grained sediments with sandstone interbeds accumulated (Bünderschists), (2) the swell region of the Briançonnais micro-continent where thick sequences of limestones built up, and (3) the Piemont ocean, a narrow transform-fault dominated ocean that opened between the Eurasian and Adriatic-African plates in Jurassic times, resulting in the formation of ophiolites. The Austroalpine and the Southalpine nappes (often referred to as Southern Alps) represent the subsided margin of the Adriatic (or Apulian) microplate, which is here considered as a promontory of the African plate (Channell, 1992).

The present-day tectonic architecture of the Swiss Alps can be characterized as doubly vergent orogen with a crystalline core of European upper crustal provenance that is exposed in the external massifs (e.g., Aar massif). It is flanked by outwardly verging thrust sheets on the northern and southern sides (Fig. 8A). On the northern side, the structurally highest unit is made up of Austroalpine nappes that structurally overlie the (meta)sedimentary sequences of the Penninic and the underlying Helvetic thrust nappes. The front of the Helvetic and Penninic units is referred to as basal Alpine thrust (Fig. 1). North of these nappes lies the Molasse Basin, a sedimentary wedge made up of clastic deposits derived from the Alps (see above). In general, this basin is bordered to the north by the Jura fold-and-thrust belt (Fig. 1). Note, however, that Molasse deposits can also be found as erosional remnants in synclines of the Jura belt. The southern side of the Alps comprises the Southalpine thrust sheets that consist of crystalline basement rocks and sedimentary units of African origin. This fold-and-thrust belt is bordered to the south by the Po Basin. Note that the most distal thrust sheets of the Southalpine nappes and especially the thrust front (Lombardic front) are covered by the deposits of the Po Basin (Fig. 8A). The north-vergent Alpine thrusts are separated from the Southalpine nappes by the north-dipping Insubric Line. This fault accommodated most of the shortening during the Oligocene and the Early Miocene by backthrusting and right-lateral slip. Movements along this fault and the associated exhumation (Fig. 8B) resulted in exposure of the high-grade Penninic crystalline core that is referred to as Lepontine dome in Alpine literature (Fig. 1). Note that the Lepontine dome is located west of the cross-section on Figure 8A.

Geodynamic evolution

The architecture of the Swiss Alps is the result of the continent-continent collision between the African and European plates that started in the Late Cretaceous. At that time, the European nappe stack was still coupled to the subducting European lithospheric mantle and lower crust. At ca. 35 Ma continent-continent collision and indentation of the Adriatic promontory of the African plate into the interface between the lower and upper European crust resulted in decoupling between the downgoing slab and the European nappe stack. As a result, the Alps started to experience vertically-directed extrusion, and exhumation rates increased to more than 1 km/My (Hurford, 1986; Schmid et al., 1989; Schlunegger & Willett, 1999) (Fig. 8B). Exhumation occurred mainly in the Lepontine region and was accommodated by backthrusting along the Insubric Line (Schmid et al., 1996). This phase of dominantly vertically-directed extrusion of deep seated rocks continued until ca. 20 Ma and resulted in widespread exposure of crystalline on the orogen surface especially in the Lepontine region (Eynatten et al., 1999). During that time, the Insubric Line and the basal Alpine Thrust (Fig. 8A) represented the Alpine front on the southern and northern sides, respectively (Gunzenhauser, 1985; Schmid et al., 1996).

At 20–18 Ma, the geodynamic processes of the Alps experienced a substantial change from dominantly vertically- to laterally-directed extrusion. This is indicated by decreasing rates of exhumation in the Lepontine, and by reduced backthrusting along the Insubric Line (Hurford, 1986; Schlunegger & Willett, 1999) (Fig 8B). At the same time, the deformation front shifted approximately 50 km towards the south (Lombardic front, Fig. 8A) to the vicinity of Milano (Pieri & Groppi, 1981; Schönborn, 1992). Similarly, on the northern side of the Alps, the deformation front shifted to the Jura fold-and-thrust belt which represents an additional ca. 50–70 km widening of the orogen. These observations indicate that a major phase of lateral orogenic growth was initiated at ca. 20 Ma, increasing the Alpine width from approximately 100 to 180 km (Schmid et al., 1996).

Note that our age assignment for the initiation of Jura deformation is controversial and by far not accepted by all Alpine geologists. We refer here to the angular unconformity between OMM deposits and Jura folds in the western Jura (Bourquin et al., 1946) that we consider an adequate observation to infer a minimum age of deformation. From there, deformation progressed towards the northeast after 11 Ma (Kälin, 1997). This implies that the Molasse was presumably in a piggy-back position during deposition of the OMM.

A further major change in the geodynamic development occurred in the Pliocene when lateral expansion and thrusting in the Jura and Southalpine nappes decreased and came to a halt (Fig. 8A). Age constraints for decreasing deformation rates in the Jura are provided by bedding-relationships between Jura folds and Neogene sediments (Bolliger et al., 1993; Becker, 2000). Similarly, in the south, the timing of the end of

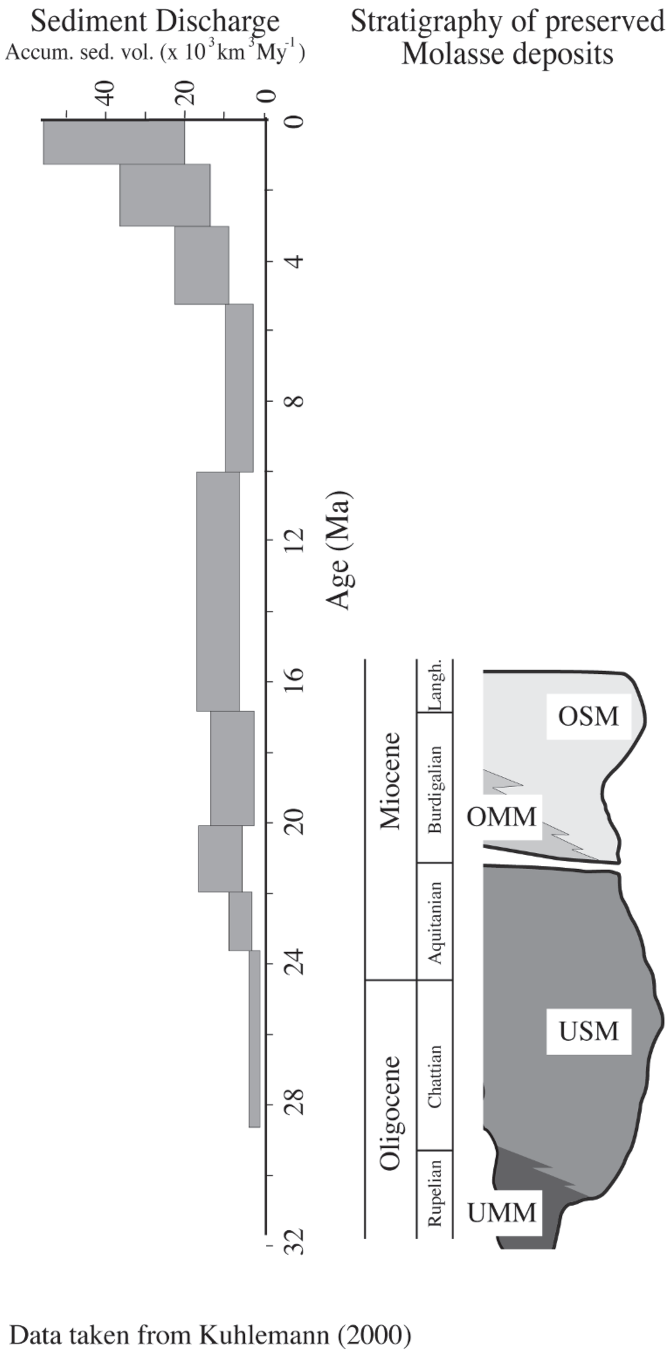

Fig. 9. Pattern of sediment discharge to the north. The figure is based on sediment budgets of Kuhlemann (2000).

Lombardic deformation (which resulted in deformation of the Southalpine nappes, see above) is constrained by cross-cutting relationships between dated strata and southern Alpine structures (Fig 8A) (Pieri & Groppi, 1981; Schumacher et al., 1996). At the same time, deformation and exhumation became focused in the region surrounding the Aar massif. This interpretation is supported by Pliocene apatite fission track ages at the eastern and western tips of the Aar massif (Michalski & Soom, 1990; Leloup et al., 2005) and by the presence of Quaternary thrust faults (Persaud & Pfiffner, 2004). Also in the Pliocene (or possibly in the Late Miocene), the Molasse basin became inverted and eroded. Specifically, Cederbom et al. (2004) reported apatite fission-track data from the Molasse basin that provided ages for the onset of cooling between 4.8 and 5.6 Ma and provided an estimate of several km of post-Miocene erosion (see above).

In summary, the Alps experienced three different stages in the geodynamic development (Fig. 8A). The first stage between ca. 35–20 Ma is characterized by predominantly vertically-directed extrusion of deep seated rocks. It was succeeded by a phase of lateral expansion of the deformation fronts to the Jura and Southern Alps, and a decrease of exhumation rates in the crystalline core. This phase of laterally-directed deformation continued until the Pliocene, when deformation stepped back into the crystalline core.

Sediment discharge, and the development of the Alpine drainage network

Sediment discharge

The calculation of sediment discharge to the north (Fig. 9) is based on sediment budgets of Kuhlemann (2000). This author compiled the volumes of preserved sediments in circum-Alpine basins (Molasse Basin, Pannonian Basin, Rheintal graben, Rhône-Bresse graben, Rhône delta, North Sea). Although Kuhlemann's work presents the most precise sediment budget for the Alps, there are three major issues that have not been resolved yet. The first one comprises differences between the chronologies of the circum-Alpine sedimentary basins. Second, the sediment budgets have not been corrected in detail for post-depositional erosion. This mainly concerns the Oligocene deposits in the thrusted Molasse (e.g., Fig. 3). Third, chemical solution of carbonate rocks which substantially contributes to erosion of the Swiss Alps (Schlunegger & Hinderer, 2003) has not been considered in the sediment budgets.

Despite these drawbacks, the Kuhlemann (2000) budget reveals that sediment discharge to the north continuously increased between Chattian and Aquitanian until a nearly stationary flux was reached at 20 Ma. Note, however that during the Burdigalian sediment discharge was reduced by ca. 30%. During the Pliocene, sediment flux increased by more than 100% and reached highest magnitudes in the Quaternary.

The Alpine drainage network

Our current knowledge about the development of the Alpine drainage network and the delineation of drainage divides between the Oligocene and the present is based on three partly independent datasets. The first one is the petrographic and

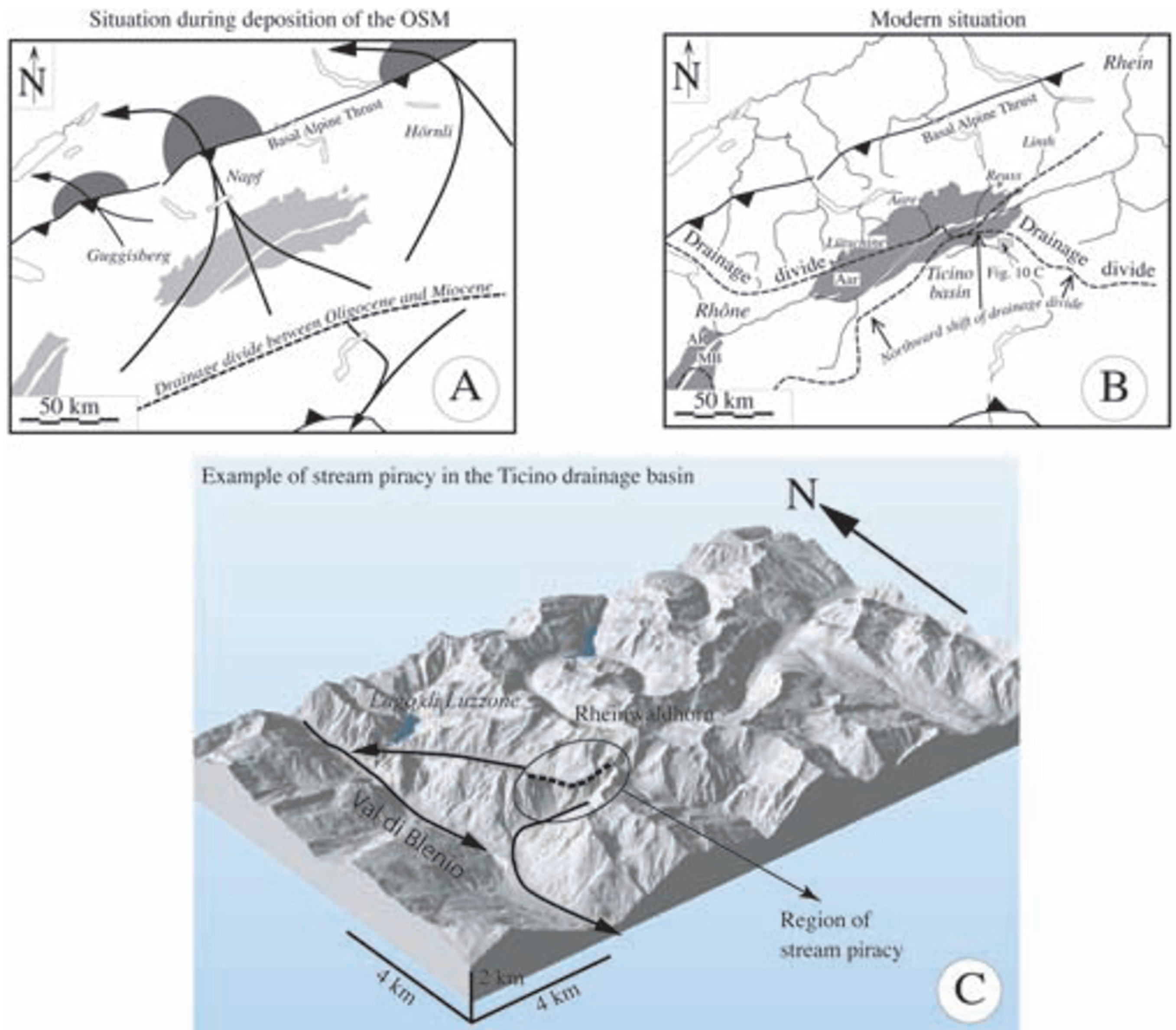

Fig. 10. (A) Illustration of drainage network during OSM time, and of (B) present-day situation that established presumably during the Pliocene. Note that the Pliocene rearrangement of the drainage network was characterized by a northward shift of the drainage divide of the south-directed rivers (arrows). Note also that since the Pliocene the core of the Central Alps has been drained by orogen-parallel systems (Rhein, Rhône). The block diagram in (C) shows an example of stream piracy in the Ticino headwaters where a W-directed tributary to the Val di Blenio cuts into the headwaters of a N-directed system (that then also becomes rerouted towards the Val di Blenio). AR=Aiguilles Rouge massif, MB=Mont Blanc massif

geochemical composition of the detrital material that yields information about the provenance of the sediment (e.g, Matter, 1964; Gasser, 1968; Stürm, 1973; Spiegel et al., 1992; von Eynatten, 2007). A second dataset are determinations of the thermo-chronometric evolution of detrital mica (^{39}Ar/^{40}Ar) and zircon/apatite crystals (fission track method). They bear information about the chronology of exhumation of the sediments that can then be compared with the pattern and rates of cooling in the hinterland (Giger, 1991; von Eynatten et al., 1999; Spiegel et al., 2000). The third piece of information are locations of the point of entries of the dispersal systems into the basin. Any shifts of these locations can be interpreted in terms of growth and/or decay of the size of the catchments. This is the case because catchments tend to adapt self similar geometries (Hovius, 1996). Hence, headward shifts of drainage divides and the associated increase of the lengths of a drainage basin will ultimately cause a lateral expansion of the catchment.

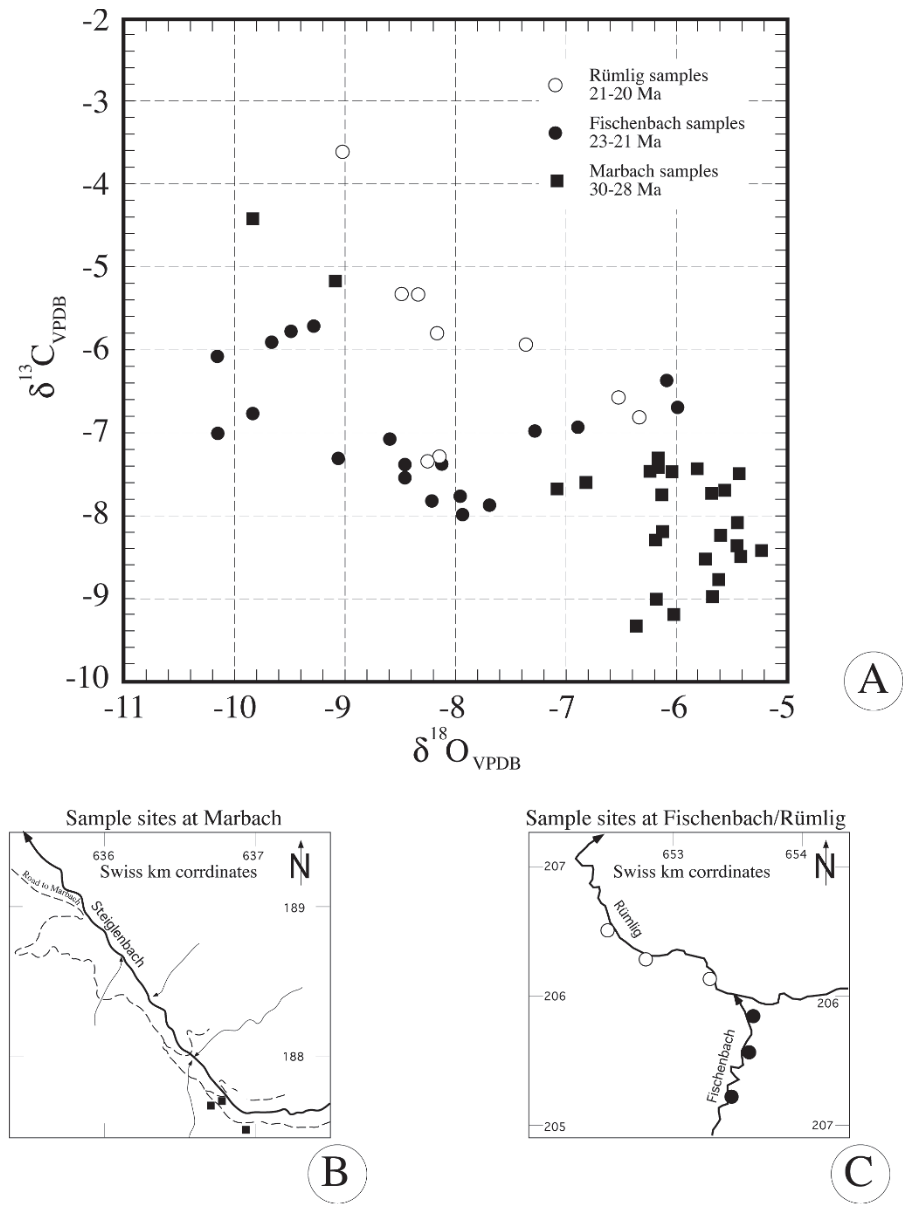

Fig. 11. (A) Isotope data of caliche nodules, and location maps of (A) Chattian and (B) Aquitanian sample sites.

Here, we use the most recent reconstruction of the drainage network of the Swiss Alps by von Eynatten et al. (1999), Spiegel et al. (2001), and Kuhlemann et al. (2001) (Fig. 10). Note, however, that we do not consider the Miocene shifts of the drainage divide between the northern and southern dispersal systems as postulated by the latter authors because of a lack of support from provenance data (Schlunegger et al., 1998; von Eynatten et al., 1999). The restorations of the Alpine drainage network resulted in the identification of three stages. During the first period, between the Chattian and the Burdigalian (Fig. 10A), the Alpine drainage network had an orogen-normal dispersal direction with a drainage divide that was located in the rear of the wedge at ca. 20–40 km distance from the Insubric Line. Also during this first stage, the petrofacies changed from predominantly sedimentary material of Austroalpine and Penninic origin, towards increased contribution of sediments from the Penninc crystalline basement. This latter unit is exposed in the rear of the orogen (Figs. 1, 8A). The modification in petrofacies suggests continuous downcutting of the Alpine rivers into the Alpine edifice and headward shift of the headwaters (Schlunegger et al., 1993). This headward expansion of catchments was most likely associated by a lateral growth of the drainage basins in order to keep a self-similar basin geometry (see paragraph above). Support for this interpretation is provided by the continuous coalescence of alluvial fans from originally 7 during the Chattian, to ca. 3 at the end of the Aquitanian (Fig. 5). This ca. 20 Ma-old situation most likely remained stationary because the petrofacies of the

Molasse deposits and the locations of the fan apexes remained stable (Fig. 6). We consider this stable situation as the second phase of drainage network evolution.

The third phase is characterized by the establishment of the present-day situation that is characterized by an orogen-parallel drainage in the core of the Central Alps (Rhône and Rhein valleys) (Fig. 10B). This modification appears to have occurred as Alpine palaeorivers were rerouted around the hinge of the growing Aar massif. Schlunegger et al. (2001) and Kühni & Pfiffner (2001a) postulated that exhumation and exposure of granites and gneisses of the Aar massif (which caused a strong contrast in the pattern of bedrock erodabilities according to Pfiffner & Kühni (2001b) was sufficient to initiate this reorganization of the drainage network. It is unclear at the moment when this third phase started. However, because the establishment of the orogen-parallel drainages (Rhein and Rhône valleys) was most likely contemporaneous with the ca. 15 km-northward shift of the Ticino headwaters (Kühni & Pfiffner, 2001a), and since evidence of stream piracy and drainage reorganization is still preserved in the Ticino basin (Fig. 10C), we assign a relatively young, possibly Pliocene, age for the initiation of this third stage. Support for a recent age is provided by Pliocene apatite fission track ages at the eastern and western tips of the Aar massif (Michalski & Soom, 1990).

The development of palaeoclimate

There are two independent datasets that bear information about the trends of paleoclimate during deposition of the Molasse. In a first dataset, Berger (1992) identified a modification in the fossiliferous record of plants that occurred somewhen during the Aquitanian. This change is characterized by the disappearance of Palms and Taxads, and the new-appearance of Pinaceae, Leguminosae and Populoids. Berger interpreted this modification to indicate a shift from a humid to a drier, more continental climate. These latter conditions most likely persisted until the Middle Miocene because the plant assemblages of an OSM site in the eastern Swiss Molasse (Öningen; Berger, 1957) are identical to those described for the Aquitanian USM in western Switzerland.

A further dataset to infer a palaeoclimate is provided by the stable isotope record of caliche nodules (Fig. 11A). These carbonate concretions commonly form in the interface between the phreatic and vadose zones of palaeosoils (Dhir et al., 2004). The stable isotope fractionation of caliche nodules are sensitive to the $\delta^{18}O$ values of precipitation (Anderson & Arthur, 1983). Similarly, the plant coverage of the soil and thus the thickness of the A-horizon affects the record of $\delta^{13}C$ in the carbonate concretions (see also Mook & de Vries, 2000). Accordingly, we measured the $\delta^{18}O$ and $\delta^{13}C$ values of caliche nodules collected from Chattian deposits (30–28 Ma, Marbach section, Fig. 11B), and from Aquitanian palaeosoils (23–20 Ma, Fischenbach and Rümlig sections, Fig. 11C). The data reveal a clear shift towards lighter oxygen and heavier carbon isotopes somewhen between 28 and 23 Ma. Specifically, $\delta^{18}O$ values from the Chattian site are between –7 and –5, and between –10.5 and –6 for the Aquitanian deposits. Similarly, $\delta^{13}C$ values span the range between –9.5 and –7.5 in Chattian, and –8 and –3.5 in Aquitanian caliche nodules, respectively. These data are interpreted to record a shift from a humid to a more continental palaeoclimate. Indeed, such climate change will cause the oxygen isotopes in the rain to become lighter (Anderson & Arthur, 1983). Similarly, a more continental climate will decrease the plant coverage (e.g., less soil derived CO_2 and thus more atmospheric CO_2) and/or the plant community (e.g., more C_4-plants in a hotter, dryer climate) of soils and hence the influence of the biosphere on the fractionation of the carbon isotopes (Cerling 1984; Cerling 1991). We then relate the shift towards heavier carbon isotopes in the caliche nodules to a decreasing plant coverage and /or changing plant community.

In summary, both the fossiliferous record of plants and the stable isotope fractionations of carbon and oxygen isotopes in caliche nodules imply that palaeoclimate conditions were humid during deposition of the Chattian USM, and dryer and more continental thereafter. Note, however, that a precise age for this climate change awaits further geochemical and palaeobontanic analyses.

It is important to emphasize here that a similar paleoclimate change has not been reported by studies from other cirum-Alpine regions. For instance, Aquitanian and Burdigalian fossil sites on the southern side of the Alps contain a substantial portion of leaves from deciduous trees, which implies a humid climate (Berger, 1957). Furthermore, palynological data from the Molasse bordering the Eastern Alps do not indicate a change in palaeoclimate (Bruch, 1998). There, palaeoclimate followed gobal trends (at least since 20 Ma, Janz & Vennemann, 2005) and appears not to have been influenced by Alpine orogeny. Thus, it is unclear at the moment whether the shift towards drier and more continental conditions as inferred for the Swiss Molasse was a local phenomen that only affected the central part of the Alps.

Discussion

Controls on the stratigraphic development of the Molasse

The facies pattern within foreland basins in general, and within the Swiss Molasse in particular, represents the integrated effect of formation rates of accommodation space through flexural downwraping, and sediment discharge into the foreland. Coupled models of orogens and foreland basins indicate that thrusting results in progradation of the facies belts in the direction of thrust movement, but that these progradational cycles may be punctuated by retrogrations (towards the orogenic front) at the onset of a loading cycle. The reason for this acyclic behavior lies in the response time of several millions of years for erosional processes to respond to phases of orogenic loading and surface uplift (Flemings & Jordan, 1990; Sinclair et al., 1991; Sinclair & Allen, 1992).

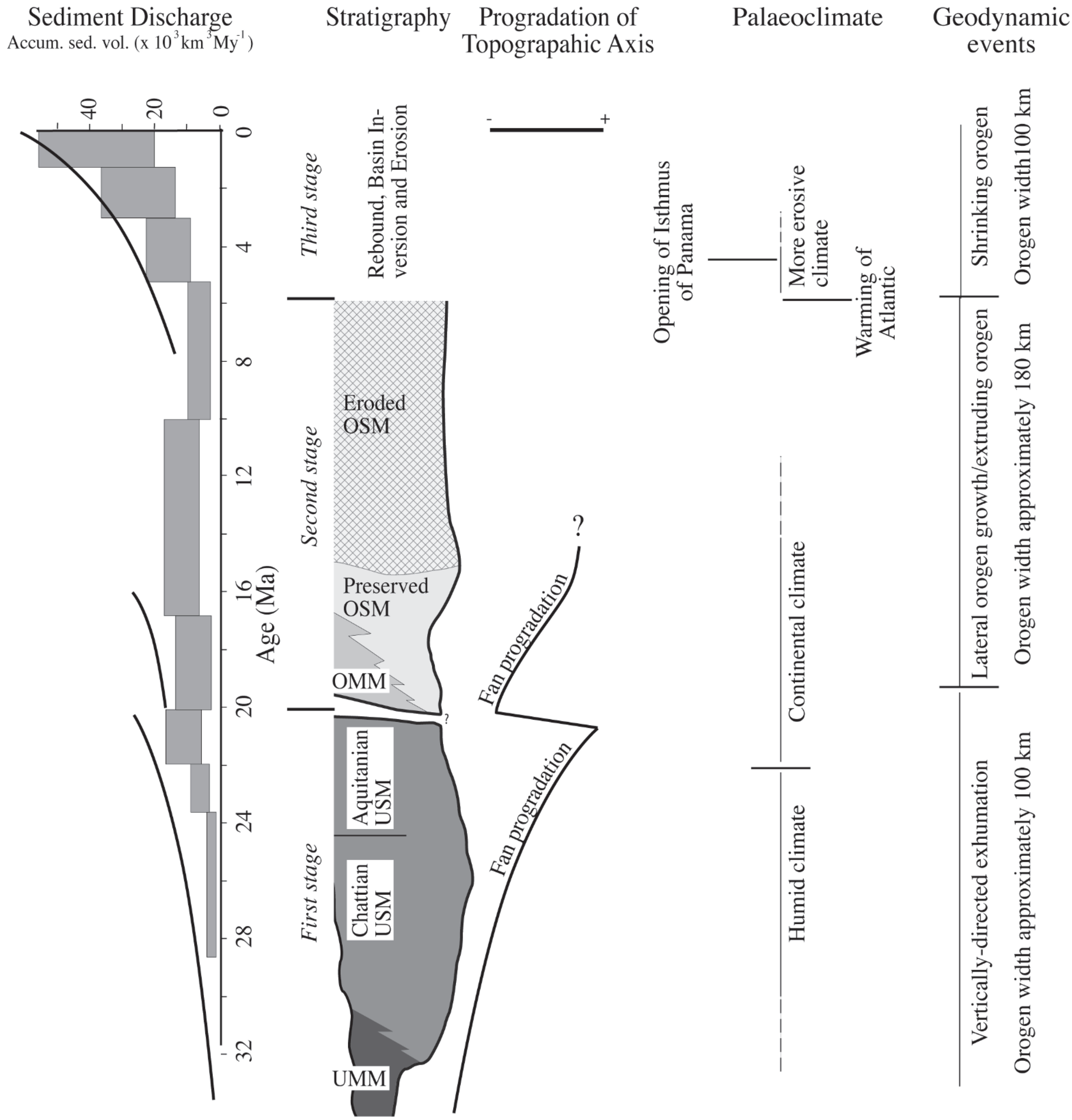

Fig. 12. Summary figure, showing (i) the pattern of sediment discharge to the north, (ii) the large-scale stratigraphic architecture of the Molasse and (iii) the trends in fan construction and in shifts of the topographic axis (that can be interpreted as changes in the relative importance of sediment discharge versus formation rates of accommodation space), (iv) palaeoclimate and (v) geodynamic scenarios in the orogen.

Here, we interpret the first regressive cycle from UMM to USM to record the coupled effect of crustal loading and erosional response. The second cycle, comprising the OMM and OSM groups, will be considered as integrated response of the Alps and the Molasse to a climate-driven decrease of surface erosion rates. Finally, we will discuss how the Late Miocene/Plicoene increase in erosional flux influenced the development of the Swiss Molasse. Hence, similar to the situation of the Alpine wedge (see next chapter), the development of the Molasse will be discussed in terms of three stages.

The *first stage* of Molasse development, i.e. the transition form UMM to USM and the subsequent progradation of depositional systems (Fig. 12), is considered here as the response of the basin to an increase in the rates of crustal thickening and surface erosion in the hinterland (see also Pfiffner et al., 2002). However, this does not mean that orogenic loads, Alpine topographies and sediment flux experienced the same temporal trends. It was argued before that at ca. 35 Ma, indentation of the Adriatic promontory of the African plate into the interface between the European upper and lower crust resulted in a phase of vertically-directed accretion of uppercrustal material and in growth of the topography. The response is the change of the foreland geometry from a relatively wide basin represented by the Helvetic Flysch (Pfiffner, 1986; Kempf & Pfiffner, 2004), to a deep trough with a high flexural curvature of the foreland plate. This latter situation is recorded by the UMM and the Chattian USM. Because the response of the sediment transfer system to surface uplift may last several millions of years, the development of the UMM and the Chattian USM was first controlled by a high ratio between rates of crustal thickening and erosional unloading. As the drainage network evolved by headward erosion and dowcutting, erosional unloading in the Alps proceeded and sediment discharge to the Molasse increased. The response is seen by the successive constructions of alluvial fans and lateral coalescence of depocentres, and by the shift of the topographic axis towards the distal basin margin (Figs. 5, 12). Ongoing erosion during the Miocene then most likely resulted in an erosional flux that balanced the accretion flux. Support for this interpretation is provided by the nearly stationary sediment discharge during the Middle and Late Miocene (an exception were the Burdigalian times as discussed below).

The *second stage*, i.e. the Burdigalian transgression of the OMM (Fig. 12), is interpreted to have resulted from the decrease in erosional flux relative to the rates of crustal accretion. This decrease most likely reached its highest effect when the St. Gallen Fm. was deposited. This was the time with the widest cross-sectional extension of the OMM sea and the deepest marine conditions. It is possible that the eustatic rise of the sea level provided a further, independent control on the establishment of marine conditions during the Burdigalian (Keller, 1989). Because this decrease in erosional flux was preceded by the shift from a humid to a drier and more continental palaeoclimate, we interpret to see here an environmental effect. Note, however, that we are aware that more detailed investigations are needed to improve the age assignment of this palaeoclimate change. Note also that exposure of crystalline rocks in the hinterland with a high erosional resistance provided a further, probably substantial contribution to the reduction in erosion rates (Schlunegger et al., 2001; Schlunegger & Simpson, 2002).

The succeeding progradational phase that resulted in the re-establishment of terrestrial conditions (OSM) is considered here to have been controlled by the augmentation in sediment flux. This increase in flux most likely occurred because widening of the orogen that started in the Burdigalian (see above) caused the Alpine source area to increase. The Jura mountains must have provided new sources for the Molasse Basin (Kuhlemann & Kempf, 2002). Note that alternative hypotheses can be extracted from the work by Naylor & Sinclair (2007). Specifically, it is possible that these variations in sediment discharge could be related to punctuated responses in thrusting in a continuously evolving orogen.

The *third stage* started at the Miocene/Pliocene boundary when sedimentation in the Molasse trough ended and when the basin became inverted and the basin fill eroded (Fig. 12). This was also the time when the sediment flux reached the highest magnitudes since the time of continent-continent collision, and when the location of active deformation shifted to the core of the Alps. In a recent paper, Cederbom et al. (2004) interpreted that a substantial contribution of at least 1–3 kilometers of basin inversion was attributed to isostatic rebound in response to a more erosive climate. It appears then that the increase in erosional flux that started somewhen between 6 and 4 Ma had two partly unrelated affects: It caused the Alps to enter a destructive stage and the locus of active deformation to shift towards the orogenic core (Willett et al., 2006, see below), but it also resulted in a net unloading of the orogen and thus in a flexural rebound of the foreland plate (Cederbom et al., 2004).

Controls on the pattern of sediment discharge, and possible feedback mechanisms between erosion and crustal accretion

Conceptual studies proposed a close linkage between lithosperic processes, surface erosion and climate during the evolution of mountain belts (e.g., Willett et al., 1993; Willett, 1999) (Fig. 13). The sensitivity of erosion to tectonics (and vice versa) is particularly acute in active orogens, where accretion of lithopsheric material leads to self-similar growth of a critical wedge at a rate that is controlled by the relative importance of crustal accretion and surface erosion (Hilley & Strecker, 2004; Whipple & Meade, 2004). An increase in crustal accretion rates at constant climate conditions, for instance, will perturb this balance, causing a critical orogen to enter a constructive state (Fig. 12B). The result is a propagation of the orogenic fronts towards more distal sides and a vertical growth of the topography in order to keep the critical self-similar geometry. Because of the vertical growth of topography, erosion rates and exhumation rates will increase and then remain at con-

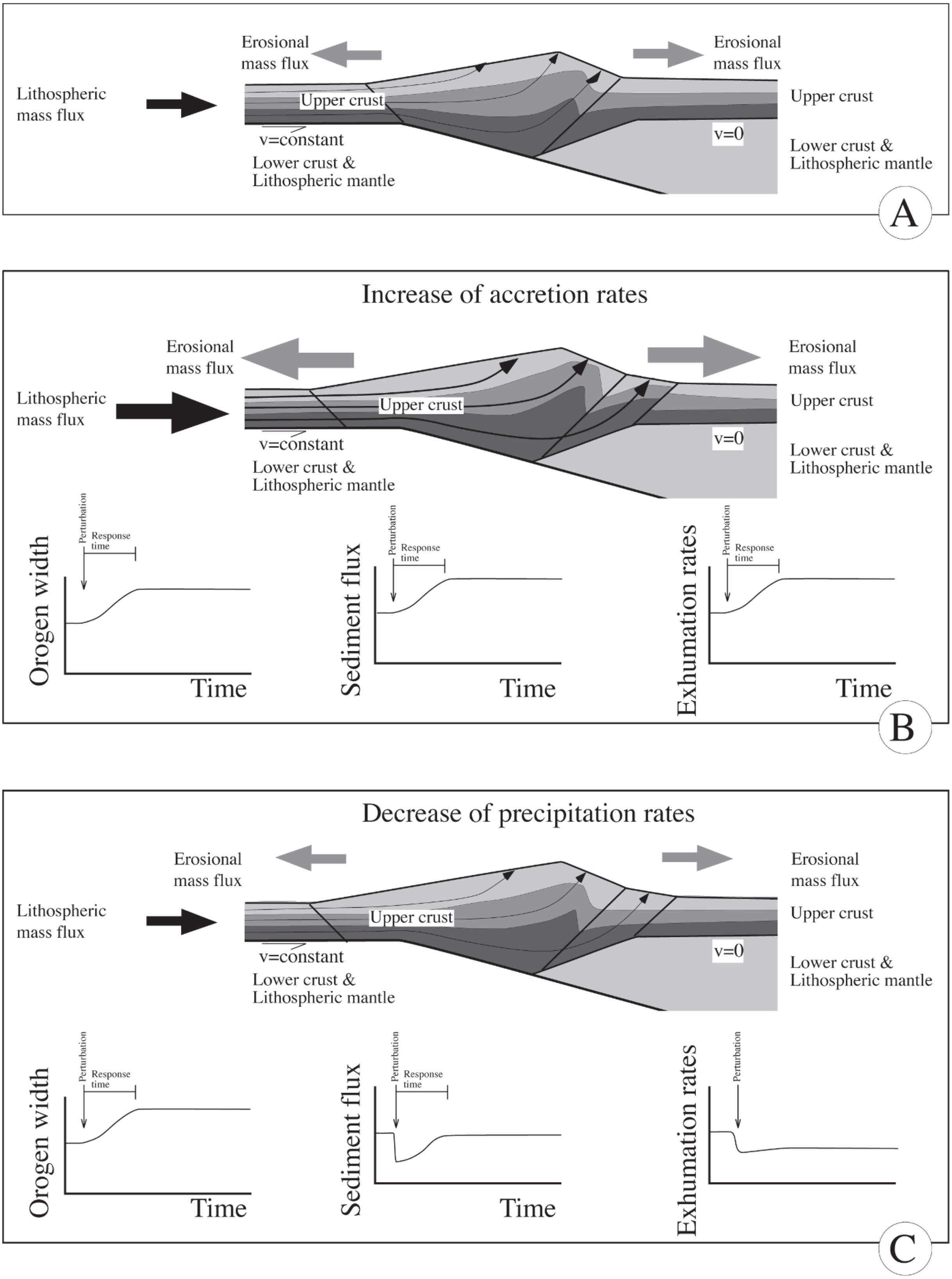

Fig. 13. Geodynamic response of self-similar critical wedge (A) to (B) an increase of crustal accretion rates at constant precipitation rates, and to (C) a decrease of precipitation rates at constant rates of crustal accretion. The concept is based on theoretical calculations of Willett et al. (1993) and Stolar et al. (2006).

stant, but higher magnitudes (Stolar et al., 2006) (Fig. 13B). The length of the response time may be five million years or even longer. It depends on the magnitude of the perturbation, and on the size of the orogen. A similar effect, but with a substantially different exhumation pattern, yields a climate-driven decrease of erosion rates at constant rates of crustal accretion (Fig. 13C). The response of a critical orogen to such a perturbation is a lateral self-similar growth. However, in contrast to the previous example, the erosional flux will first decrease, and then increase to the magnitudes prior to the perturbation. This increase occurs because erosion operates at a successively larger surface as the orogen widens. The orogen will enter a stable and steady situation when the accretionary flux will be balanced by the erosional flux. Note, however, at this new stage exhumation rates will be lower than prior to the perturbation. Hence, the response of a climate-driven lateral growth of a critical orogen is a change from predominantly vertically- to laterally-driven exhumation (Stolar et al., 2006). In a final case, an increase in the erosional flux larger than the accretionary flux will destroy the critical topography, leading to a smaller active wedge where deformation focuses in the core of the orogen to restore the critical taper. The result is a change towards a more vertically-directed exhumation in the orogen core.

According to these conceptual models, we interpret the augmentation in sediment flux during the *first stage* of Alpine evolution, i.e. between ca. 35 and 20 Ma (Figs. 8, 12), to represent the response of the sediment transfer system to crustal thickening. During this time interval, indentation of the Adriatic promontory of the African plate into the interface between the upper and lower crust of the European continental plate resulted in a change from predominantly subduction to accretion of uppercrustal material (Schmid et al., 1996). The result is a net accretion of crust into the orogen and a predominantly vertical growth of the Alpine edifice and the topography (Fig. 8A). The response on the surface was an expansion of the drainage network towards the rear of the orogen and downcutting. The data that is consistent with this interpretation is an increase in sediment discharge, a shift in the petrographic composition of conglomerates towards more crystalline constituents with sources in the rear of the Alps, lateral coalescence of alluvial fans, and high exhumation rates indicating a vertically-directed exhumation (Figs. 8B, 12, 13B).

The *second stage* started in the Burdigalian and lasted until the end of the Miocene (Figs. 8, 12). It is characterized by a lateral expansion of the wedge by ca. 100% as the southern Alps (Lombardic phase of deformation) and the Jura mountains became incorporated into the wedge (Fig. 8A). This growth of the deforming wedge was associated by a decrease of exhumation rates and sediment flux (Figs. 8B, 9). It implies a change from predominantly vertically-directed exhumation to lateral extrusion. Here, we do not consider an increase in crustal accretion rates to have initiated this second stage because such a scenario would have ultimately resulted in an increase in exhumation rates and sediment discharge (see above). We rather consider the climate-driven decrease in surface erosion rates to have commenced this second stage of growth (which is consistent with the theoretical concepts presented above). Because the distal shift of the deformation fronts also enhanced the area on which erosion operated (though at lower magnitudes), sediment flux most likely increased until accretionary flux was balanced by the erosional flux. This appears to have been the case at end of the Burdigalian when the erosional flux reached similar magnitudes as at the end of the Aquitanian, and when terrestrial conditions were re-establihsed (deposition of OSM, Fig. 12).

It is important to emphasize here that this palaeoclimate scenario for the lateral orogenic growth is by no means accepted by all Alpine geologists. Alternative models present a tectonic driving force. For instance, it was proposed that the lateral orogenic growth occurred because crustal accretion rates increased relative to erosion rates (Beaumont et al., 1996). Such a scenario may have occurred if the proportion of mass subducted compared to that accreted decreased (e.g., Beaumont et al., 1996). This was the case for the Alps when indentation started at ca. 35 Ma, but it is probably too early to explain the Miocene phase of lateral orogenic growth. A second alternative possibility is that lateral spreading may have been caused by a change in rheology, for example due to thermal weakening (e.g., Dewey, 1988) or to interaction with pre-existing zones of mechanical weakness (e.g., Pfiffner et al., 2000).

The *third stage* of Alpine development started in the Late Miocene or early Pliocene (Figs. 8, 12). At that time, thrusts beneath the Po Plain became sealed by undeformed Pliocene (Pieri & Groppi, 1981), shortening in the Jura decreased (Becker, 2000), the Molasse basin became inverted and eroded (Cederbom et al., 2004), and active deformation started to focus in the core of the Alps where Quaternary thrusts were mapped (Persaud & Pfiffner, 2004). At the same time, sediment flux from the Alps increased to reach the highest magnitudes since the time of continent-continent collision. It caused the Alps to enter a destructive stage and the locus of active deformation to shift towards to the orogenic core (Willett et al., 2006, see below), but it also resulted in a net unloading of the orogen and thus in a flexural rebound of the foreland plate (Cederbom et al., 2004). This third stage was considered by Willett et al. (2006) to represent the situation when the Alps changed from construction to destruction. According to their argumentation, an erosional flux that was possibly larger than the accretionary flux will destroy the critical topography, leading to a smaller active wedge where deformation focuses in the core of the orogen to restore the critical taper. Willett et al. (2006) argued that this Late Miocene/Pliocene increase in erosional flux might have been initiated by the base level fall associated with the Messinian salinity crises in the Mediterranean. More important, however, appears the persistence of high sediment yields into the Pliocene. Willett et al. (2006) considered the end of the late Miocene glacial period as possible control. In contrast, Cederbom et al. (2004) argued that a shift to wetter climate on continental Europe was marked by the onset of the Gulf Stream related to the closure of the Isthmus of Panama (Fig. 12).

Note that the scenarios of a climate-driven increase in erosional mass flux and the geodynamic implications are debated. Alternative hypothesis comprise deep crustal processes as driving forces. For instance, Kuhlemann et al. (2001) thought that the Pliocene increase in sediment discharge might be a combined effect of underplating and granulatisation at deep crustal levels followed by glaciation. An other possible control is slab breakoff that has for instance been used to explain the Rupelian/Chattian increase in sediment flux (Sinclair, 1997). However, we propose that flexural rebound related slab breakoff is inconsistent with the shrinking orogen hypothesis of Willett et al. (2006).

Implications for further studies

We propose that the resolution of the data about the lithospheric development of the Alps and the stratigraphic evolution of the Swiss Molasse is adequate to relate the history of the foreland to Alpine geodynamic events, and to discuss about possible feedback mechanisms between environmental effects and lithospheric processes. However, further progress in our understanding of the Molasse requires a substantial downscaling of research. Specifically, the sedimentological and stratigraphic response of the USM to the change in palaeoclimate has not yet been explored in sufficient detail. Such a shift in palaeoclimate will affect the rates and the pattern of water discharge in fluvial channels (e.g., Molnar, 2001). We anticipate adjustments in the cross-sectional geometries of channels, in the composition of the mechanical loads (bedload and suspended loads), and in the flow patterns. Similarly, because of exposure of the crystalline core in the Alps during the Aquitanian, the palaeoclimate change also altered the rates and the nature of Alpine weathering, which, in turn, probably modified the sedimentary loads in the channel network in general and the ratio between suspended loads and bedloads in particular. Besides adjustments of cross-sectional geometries of channels and the internal organization of bedforms, we propose a change in the stacking pattern of channels. Specifically, magnitudes of sedimentary loads and ratios between suspension and bedloads exert an important control on avulsion rates, and therefore on the lateral and vertical distribution of channel sandstones (Slingerland & Smith, 1998). The expected result is a different architecture in the topographic axis between the Chattian and Aquitanian USM deposits.

Summary and Conclusions

The availability of a high-resolution temporal framework for foreland basin deposits has allowed to identify three partly unrelated stages in the geodynamic evolution of the Alps and the sedimentary response in the Molasse Basin. During the first stage between ca. 35 and 20 Ma, the basin width, the dispersion direction, the pattern of subsidence rates and the location of the topographic axis were most likely controlled by the ratio between rates of deep crustal processes leading to crustal thickening, and surface processes resulting in redistribution of mass from the orogen to the adjacent foreland. Specifically, indentation and crustal growth between the Eocene and the Oligocene caused an increase in the rates of crustal accretion and surface erosion. As a result, the basin became overfilled as indicated by the stratigraphic change from marine to terrestrial conditions (evolution from UMM to USM). However, because the response time of erosional processes to crustal dynamics is in the range of several Ma, the orogen experienced a net growth until the end of the Oligocene. As a result, the Molasse Basin subsided at high rates causing the topographic axis to shift to the proximal basin border. In addition, km-thick alluvial fan deposits with dm-large gravels established at the proximal basin border. During the Aquitanian, however, ongoing erosion and downcutting in the hinterland caused the ratio between the rates of rock uplift and erosion to decrease. As a result, the dispersal systems prograded into the basin, the topographic axis shifted towards the distal basin border, and the pebble size of conglomerates at proximal positions decreased to the cm- scale.

This relationship changed at the beginning of the second stage at ca. 20 Ma when palaeoclimate became more continental, and when the crystalline core became exposed in the orogen. This modification was preceded by a change in palaeoclimate from humid to more continental conditions. The effect was a decrease in the erosional efficiency of the Swiss Alps and hence a reduction of sediment discharge to the Molasse Basin. As a result the basin became underfilled and marine conditions of the OMM established. The decrease in erosional efficiency as outlined above probably played an important role in the initiation of a major phase of lateral orogenic growth (deformation of the Southern Alps, and the Jura Mountains some Ma later). It was suggested that the effect was a change of the deformation of the orogen from vertically- to mainly horizontally-directed extrusion.

Similar to the previous situation, initiation of the last stage most likely had a climatic control. This third stage of Alpine development started in the Late Miocene or early Pliocene at a time when climate possibly became more erosive. The result was an increase in sediment flux to the highest magnitudes since the time of continent-continent collision. This increase in erosional flux had two partly unrelated effects: It caused the Alps to enter a destructive stage and the locus of active deformation to shift towards to the orogenic core, but it also resulted in a net unloading of the orogen and thus in a flexural rebound of the foreland plate.

In summary, the available chronological record allows to propose possible causal links and feedback mechansims between Alpine geodynamics, climate, exposed bedrock lithologies and sedimentary processes at large spatial and temporal scales. However, pending questions require a more detailed chronological and spatial framework for the Molasse deposits than is currently available. These comprise the search for pos-

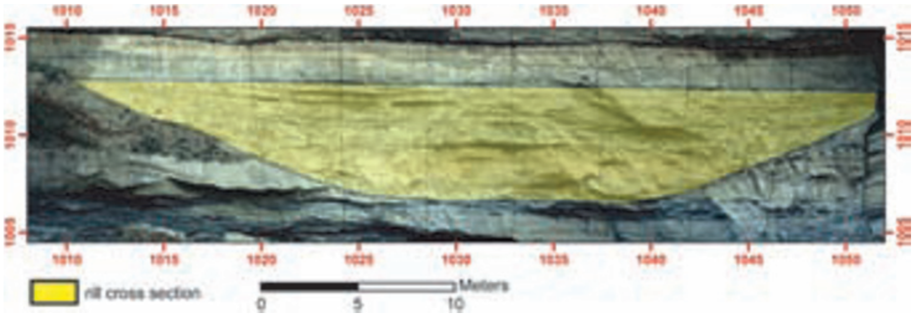

Fig. 14. Orthorectified image generated from overlapping stereo images of a palaeo rill cross-section for OSM at Wolhusen/Entlebuch taken with a Wild APK1 metric camera. Flow direction was perpendicular to the outcrop wall. The cross section of the rill is highlighted in the image and measures 178 m^2. Flow velocity in the rill can be inferred from the size of transported pebbles. Palaeodischarge can then be calculated as the product of cross section and flow velocity.

sible controls on the stratal architecture at the outcrop scale. For instance, there is a consensus that the stacking pattern of lithofacies is controlled by lateral shifts of distributary channels in terrestrial and marine environments. However, it has been unclear whether these shifts have been driven by local instabilities in sediment flux (autocyclic control), or by climate-driven variations in the relative importance of sediment production by weathering on hillslopes, and sediment export in channels (allocyclic control). For instance, the inferred climate change at the Chattian/Aquitanian boundary should be seen by an equivalent modification in the channel geometries. We see a benefit in measuring cross-sectional geometries of channels perpendicular to the flow direction (e.g., Fig. 14), and in identifying the granulometric composition of channel fills. These information can then be used to calculate the flow strength during transport and deposition of sediment, which, in turn, will yield information about water discharge (Allen, 1997). If these data are established for the whole basin and for the whole time span of Molasse accumulation, we will be able to provide a more detailed picture of palaeorunoff, runoff variabilites and controls thereof. Hence, this implies a substantial down-scaling of both space and time during future research activities.

REFERENCES

Allen, P.A. 1984: Reconstruction of ancient sea conditions with an example from the Swiss Molasse. Marine Geology 60, 437–455.

Allen, P.A. 1997: Earth Surface Processes. Blackwell Science, Oxford, 404 pp.

Allen, P.A., Mange, M., Matter, A. & Homewood, P. 1985: Dynamic palaeogeography of the open Burdigalian seaway, Swiss Molasse basin. Eclogae geologicae Helevetiae 78, 351–381.

Anderson, T. & Arthur, M. 1983: Stable isotopes of oxygen and carbon and their application to sedimentologic and paleoenvironmental problems. In: Arthur, M., Anderson, T., Kaplan, I., Veizer, J. & Land, L. (Eds.): Stable isotopes in sedimentary geology. SEPM short courses 10, 151 pp.

Beaumont, C., Ellis, S., Hamilton, J. & Fullsack, P. 1996: Mechanical model for subduction-collision tectonics of Alpine-type compressional orogens. Geology 24, 675–678.

Becker, A. 2000: The Jura Mountains – An active foreland fold-and-thrust belt? Tectonophysics 321, 381–406.

Berger, W. 1957: Untersuchungen an der obermiozänen (sarmatischen) Flora von Gabbro (Monti Livornesi) in der Toskana, ein Beitrag zur Auswertung tertiärer Blattforen für die Klima- und Florengeschichte. Palaeontographica Italica 51, 96 pp.

Berger, J.P. 1983: La transgression de la molasse marine supérieure (OMM) en Suisse occidentale. Münchner Geowissenschaftliche Abhandlungen A5, 207 pp.

Berger, J.P. 1992: Paléontologie de la Molasse de Suisse Occidentale, taxonomie, biostratigraphie, paléoecologie, paléogéographie et paléoclimatologie. Habilitation thesis, Fribourg, Univ. Fribourg, 405 pp.

Berger, J.P., Reichenbacher, B., Becker, D., Grimm, M., Grimm, K., Picot, L., Storni, A., Pirkenseer, C. & Schaefer, A. 2005a: Eocene-Pliocene time scale and stratigraphy of the Upper Rhine Graben (URG) and the Swiss Molasse Basin (SMB). International Journal of Earth Sciences 94, 711–731.

Berger, J.P., Reichenbacher, B., Becker, D., Grimm, M., Grimm, K., Picot, L., Storni, A., Pirkenseer, C. & Schaefer, A. 2005b: Paleogeography of the Upper Rhine Graben (URG) and the Swiss Molasse Basin (SMB) from Eocene to Plicoene. International Journal of Earth Sciences 94, 697–710.

Bieg, U. 2005: Palaeooceanographic modeling in global and regional scale: An example from the Burdigalian seaway, Upper Marine Molasse (Early Miocene). PhD thesis, Univ. Tübingen, 107 pp.

Bolliger, T., Engesser, B. & Weidmann, M. 1993: Première découverte de mammifères pliocènes dans le Jura neuchâteois. Eclogae Geologicae Helvetiae 86, 1031–1068.

Bourquin, Ph., Suter, H. & Fallot, P. 1946: Geologischer Atlas der Schweiz, Altasblatt 15, Blätter 114 Biaufond, 116 La Ferrière, 115 Les Bois, 117 St. Imier. Geologische Kommission der Schweizerischen Naturforschenden Gesellschaft. Landesgeshydrologie und -geologie, Wabern (Bern).

Bruch, A.A. 1998: Palynologische Untersuchungen im Oligozän Sloweniens – Paläo-Umwelt und Paläoklima im Ostalpenraum. Tübinger Mikropaläontologische Mitteilungen 18, 193 pp.

Burbank, D.W., Engesser, B., Matter, A. & Weidmann, M. 1992: Magnetostratigraphic chronology, mammalian faunas, and stratigraphic evolution of the Lower Freshwater Molasse. Eclogae geologicae Helvetiae 85, 399–431.

Cederbom, C., Sinclair, H., Schlunegger, F. & Rahn, M. 2004: Climate induced rebound and exhumation of the European Alps. Geology 32, 709–712.

Cerling, T.E. 1984: The stable isotopic composition of modern soil carbonate and its relationship to climate. Earth and Planetary Science Letters 71, 229–240.

Cerling, T.E. 1991: Carbon dioxide in the atmosphere: Evidence from Cenozoic and Mesozoic paleosols. American Journal of Science 291, 377–400.

Channell, J.E.T. 1992: Paleomagnetic data from Umbria (Italy): implications for the rotation of Adria and Mesozoic apparent polar wander paths. Tectonophysics 216, 365–378.

Chen, J., Burbank, D.W., Scharer, K.M., Sobel, E., Yin, J., Rubin, C. & Zhao, R. 2002: Magnetochronolgy of the upper Cenozoic strata in the southwestern Chinese Tian Shan; rates of Pleistocene folding and thrusting. Earth and Planetary Science Letters 195, 113–130.

Dewey, J.F. 1988: Extensional collapse of orogens. Tectonics 7, 1123–1139.

Dhir, R.P., Tandon, S.K., Sareen, B.K., Ramesh, R., Rao, T.K.G., Kailath, A.J. & Sharma, N. 2004: Calcretes in the Thar desert: genesis, chronology and palaeoenvironment. Proceedings of the Indian Academy of Sciences-Earth and Planetary Sciences 113, 473–515.

Diem, B. 1985: Analytical method for estimating palaeowave climate and water depth from wave ripple marks. Sedimentology 32, 705–720.

Diem, B. 1986: Die untere Meeresmolasse zwischen der Saane (Westschweiz) und der Ammer (Oberbayern). Eclogae Geologicae Helvetiae 79. 493–559.

Engesser, B. 1990: Die Eomyidae (Rodentia, Mammalia) der Molasse der Schweiz und Savoyens. Systematik und Biostratigraphie. Schweizerische Paläontologische Abhandlungen 112, 144 pp.

Eynatten, von, H., Schlunegger, F., Gaupp, R. & Wijbrans, J.R. 1999: The exhumation of the Lepontine: Evidence from 40Ar/39Ar laserprobe dating of detrital white micas from the Swiss Molasse Basin. Terra Nova 11, 284–289.

Eynatten, von, H. 2007: Heavy Minerals in the Swiss Molasse Basin: Occurrence, Frequency, Chemistry and Thermochronology. In: Mange, M. & Wright, P. (Eds): Heavy minerals in use. Developments in Sedimentology, Elsevier. In press.

Flemings, P.B. & Jordan, T.E. 1990: Stratigraphic Modeling of Foreland Basins: Interpreting Thrust Deformation and Lithospheric Rheology. Geology 18, 430–434.

Gasser, U. 1968: Die innere Zone der subalpine Molasse des Entlebuchs (Kt. Luzern), Geologie und Seidmentologie. Eclogae Geologicae Helvetiae 61, 229–313.

Giger, M. 1991: Geochronologische und petrographische Studien an Geröllen und Seidmenten der Gonfolite Lombarda Gruppe (Südschweiz und Norditalien) und ihr Vergleich mit dem alpinen Hinterland. Unpublished PhD thesis, University of Bern, 227 pp.

Gunzenhauser, B.A. 1985: Zur Sedimentologie und Paläogeographie der oligo-micaenen Gonfolite Lombarda zwischen Lago Maggiore und der Brianza. Beiträge zur geologischen Karte der Schweiz 159, Birkhäuser, Basel. 114 pp.

Hilley, G.E. & Strecker, M.R. 2004: Steady state erosion of critical Coulomb wedges with applications to Taiwan and the Himalaya. Journal of Geophysical Research 109, doi:10.1029/2002jb002284.

Horton, B.K. & DeCelles, P.G. 2001: Modern and ancient fluvial megafans in the foreland basin system of the Central Andes, southern Bolivia; implications for drainage network evolution in fold-and-thrust belts. Basin Research 13, 43–63.

Hovius, N. 1996: Regular spacing of drainage outlets from linear mouontain belts. Basin Research 8, 29–44.

Hurford, A.J. 1986: Cooling and uplift patterns in the Lepontine Alps South Central Switzerland and an age of vertical movement on the Insubric fault line. Contributions to Mineralogy and Petrology 93, 413–427.

Janz, H. & Vennemann, T.W. 2005: Isotopic composition (O, C, Sr, and Nd) and trace element ratios (Sr/Ca, Mg/Ca) of Miocene marine and brackish ostracods from North Alpine foreland deposits (Germany and Austria) as indicators for palaeoclimate. Palaeogeography, Palaeoclimatology, Palaeoecology 225, 216–247.

Jordan, T.E., Schlunegger, F. & Cardozo, N. 2001: Unsteady and spatially variable evolution of the Neogene Andean Bermejo foreland basin, Argentina. Journal of South American Earth Sciences 14, 775–798.

Kälin, D. 1997: Litho- und Biostratigraphie der mittel- bis obermiozänen Bois de Raube-Formation (Nordwestschweiz). Eclogae Geologicae Helvetiae 90, 97–114.

Keller, B. 1989: Fazies und Stratigraphie der Oberen Meeresmolasse (Unteres Miozän) zwischen Napf und Bodensee. Unpublished PhD thesis, University of Bern, 277 pp.

Keller, B., Bläsi, H.R., Platt, N.H., Mozley, P.S. & Matter, A. 1990: Sedimentäre Architektur der distalen Unteren Süsswassermolasse und ihre Beziehung zur Diagenese und den petrophysikalischen Eigenschaften am Beispiel der Bohrungen Langenthal. Geologische Berichte der Landeshydrologie und –geologie 13, 100 pp.

Kempf, O., Bolliger, T., Kälin, D., Engesser, B. & Matter, A. 1997: New magnetostratigraphic calibration of early to middle Miocene mammal biozones of the North Alpine foreland basin. In: Aguilar, J.P., Legendre, S. & Michaux, J. (Eds): Actes du Congrès BichroM'97. Mém. Trav. EPHE, Inst. Montpellier 21: 547–561.

Kempf, O., Matter, A., Burbank, D.W. & Mange, M. 1999: Depositional and structural evolution of a foreland basin margin in a magnetostratigraphic framework; the eastern Swiss Molasse Basin. In: Engi, M., Matter, A., Pfiffner, O.A., Trümpy, R. & Berger, W.H. (Eds.): Geological dynamics of alpine-type mountain belts; ancient and modern. International Journal of Earth Sciences 88, 253–275.

Kempf, O. & Pfiffner, O.A. 2004: Early Tertiary evolution of the North Alpine foreland basin of the Swiss Alps and adjoining areas. Basin Research 16, 549–567.

Kempf, O. & Pross, J. 2005: The Lower Marine to Lower Freshwater Molasse transition in the northern Alpine foreland basin (Oligocene; central Switzerland – south Germany): age and geodynamic implications. International Journal of Earth Sciences 94, 160–171.

Kempf, O. 2006: Long-term controls on stratigraphy deduced from sedimentary archives: Case studies from the Palaeocene-Miocene North Alpine forleand basin and Upper Triassic South Germanic basin. Habilitation thesis, TU Braunschweig.

Kuhlemann, J. 2000: Post-collisional sediment budget of circum-Alpine basins (Central Europe). Memorie degli Istituti di Geologia e Mineralogia dell' Universita di Padova 52, 91 pp.

Kuhlemann, J. & Kempf, O. 2002: Post-Eocene evolution of the North Alpine Foreland Basin and its response Alpine tectonics. Sedimentary Geology 152, 45–78.

Kuhlemann, J., Frisch, W., Dunkl, I. & Szekely, B. 2001: Quantifying tectonic versus erosive denudation by the sediment budget; the Miocene core complexes of the Alps. Tectonophysics 330, 1–23.

Kühni, A. & Pfiffner, O.A. 2001a: Drainage pattern and tectonic forcing: a model study for the Swiss Alps. Basin Research 13, 169–197.

Kühni, A. & Pfiffner, O.A. 2001b: The relief of the Swiss Alps and adjacent areas and its relation to lithology and structure: topographic analysis from a 250-m DEM. Geomorphology 41, 285–307.

Leloup, P.H., Arnaud, N., Sobel, E.R. & Lacassin, R. 2005: Alpine thermal and structural evolution of the highest external crystalline massif: The Mont Blanc. Tectonics 24, doi:10.1029/2004TC001676.

Martel, A.T., Allen, P.A. & Slingerland, R.L. 1994: Use of tidal-circulation modeling in palaeogeographical studies: an example from the Tertiary of the Alpine perimeter. Geology 22, 925–928.

Matter, A. 1964: Sedimentologische Untersuchungen im östlichen Napfgebiet (Entlebuch – Tal der Grossen Fontanne, Kt. Luzern). Eclogae Geologicae Helvetiae 57, 315–428.

Matter, A., Homewood, P., Caron, C., Rigassi, D., Van Stujivenberg, J., Weidmann, M. & Winkler, W. 1980: Flysch and molasse of western and central Switzerland. In: Trümpy, R. (ed.): Geology of Switzerland, a guidebook, Part B, Excursions. Schweizerische Geologische Kommission, 261–293.

Mazurek, M., Hurford, A. & Leu, W. 2006: Unravelling the multi-stage burial history of the Swiss Molasse basin: integration of apatite fission track, vitrinite reflectance and biomarker isomerisation analysis. Basin Research 18, 27–50.

Michalski, I. & Soom, M. 1990: The Alpine thermo-tectonic evolution of the Aar and Gotthard massifs, Central Switzerland: Fission-track ages on zircon and apatite and K-Ar mica ages. Schweizerische Mineralogische und Petrographische Mitteilungen 70, 373–387.

Molnar, P. 2001: Climate change, flooding in arid environments, and erosion rates. Geology 29, 1071–1074.

Mook, W. & de Vries, J.J. 2000: Environmental isotopes in the hydrological cycle, principles and applications, Volume I: Introduction-Theory, Methods, Review. IAEA publications, 271 pp.

Naylor, M. & Sinclair, H. 2007: Punctuated thrust deformation in the context of doubly vergent thrust wedges: Implications for the localization of uplift and exhumation. Geology 35, 559–562.

Persaud, M. & Pfiffner, O.A. 2004: Active deformation in the eastern Swiss Alps: post-glacial faults, seismicity and surface uplift. Tectonophys 385, 59–84.

Pfiffner, O.A. 1986: Evolution of the north Alpine foreland basin in the central Alps. In: Allen, P.A. & Homewood, P. (Eds.): Foreland basins. International Association of Sedimentologists Special Publication 8, 219–228.

Pfiffner, O.A., Ellis, S. & Beaumont, C. 2000: Collision tectonics in the Swiss Alps; insight from geodynamic modelling. Tectonics 19, 1065–1094.

Pfiffner, O.A., Schlunegger, F. & Buiter, S. 2002: The Swiss Alps and their peripheral foreland basin: stratigraphic response to deep crustal processes. Tectonics 21, 3.1–3.16.

Pieri, M. & Groppi, G. 1981: Subsurface geological structure of the Po Plain. Programma Finale del Consilio Nazionale die Geodinamica delle Ricerde, Rom. 414pp.

Platt, N.H. & Keller, B. 1992: Distal alluvial deposits in a foreland basin setting – the Lower Freshwater Molasse (Lower Miocene), Switzerland: Sedimentology, architecture and palaeosols. Sedimentology 39, 545–565.

Schlunegger, F., Matter, A. & Mange, M. 1993: Alluvial fan sedimentation and structure of the southern Molasse basin margin, Lake Thun area, Switzerland. Eclogae Geologicae Helvetiae 86, 717–750.

Schlunegger, F., Burbank, D.W., Matter, A., Engesser, B. & Mödden, C. 1996: Magnetostratigraphic calibration of the Oligocene to Middle Miocene (30–15 Ma) mammal biozones and depositional sequences of the Swiss Moalsse Basin. Eclogae Geologicae Helvetiae 89, 753–788.

Schlunegger, F., Jordan, T.E. & Klaper, E.M. 1997a: Controls of erosional denudation in the orogen on foreland basin evolution: The Oligocene central Swiss Molasse Basin as an example. Tectonics 16, 823–840.

Schlunegger, F., Leu, W. & Matter, A. 1997b: Sedimentary sequences, seismic facies, subsidence analysis, and evolution of the Burdigalian Upper Marine Molasse group, central Switzerland. AAPG Bulletin 81, 1185–1207.

Schlunegger, F., Slingerland, R. & Matter, A. 1998: Crustal thickening and crustal extension as controls on the evolution of the drainage network of the central Swiss Alps between 30 Ma and the present: constraints from the stratigraphy of the North Alpine Foreland Basin and the structural evolution of the Alps. Basin Research 10, 197–212.

Schlunegger, F. 1999: Controls of surface erosion on the evolution of the Alps; constraints from the stratigraphies of the adjacent foreland basins. In: Engi, M., Matter, A., Pfiffner, O.A., Trümpy, R. & Berger W.H. (Eds.): Geological dynamics of alpine-type mountain belts; ancient and modern. International Journal of Earth Sciences 88, 285–304.

Schlunegger, F., Melzer, J. & Tucker, G. 2001: Climate, exposed source rock lithologies, crustal uplift and surface erosion – a theoretical analysis calibrated with data from the Alps/North Alpine Foreland Basin system. International Journal of Earth Sciences 90, 484–499.

Schlunegger, F. & Willett, S.D. 1999: Spatial and temporal variations in exhumation of the Central Swiss Alps and implications for exhumation mechanisms. In: Brandon, M. & Willett, S.D. (Eds.): Exhumation processes: normal faulting, ductile flow, and erosion. Geological Society of London Special Publication 154, 157–180.

Schlunegger, F. & Simpson, G. 2002: Possible erosional control on lateral growth of the European Central Alps. Geology 30, 907–912.

Schlunegger, F. & Hinderer, M. 2003: Pleistocene/Holocene climate change, re-establishment of fluvial drainage network and increase in relief in the Swiss Alps. Terra Nova 15, 88–95.

Schmid, S.M., Aeberli, H.R., Heller, F. & Zingg, A. 1989: The role of the Periadriatic Line in th etectonic evolution of the Alps. In: Coward, M., Dietrich, D. & Park, R. (Eds.): Alpine tectonics: Geological Society of London Special Publication 45, 153–171.

Schmid, S.M., Pfiffner, O.A., Froitzheim, N., Schönborn, G. & Kissling, E. 1996: Geophysical-geological transect and tectonic evolution of the Swiss-Italian Alps. Tectonics 15, 1036–1064.

Schönborn, G. 1992: Alpine tectonics and kinematic models of the central Southern Alps. Memorie di Scienze Geologiche (Padova) 44, 229–393.

Schumacher, M.E., Schönborn, G., Bernoulli, D. & Laubscher, H.P. 1996: Rifting and collision in the Southern Alps. In: Pfiffner, O.A., Lehner, P., Heitzmann, P., Müller, S. & Steck, A. (Eds.): Deep structure of the Swiss Alps: Results of the National Research Program 20 (NRP-20), Birkhäuser, 186–204.

Sinclair, H.D., Coakley, B.J., Allen, P.A. & Watts, A.B. 1991: Simulation of foreland fasin stratigraphy using a diffusion model of Mountain belt uplift and erosion: an example from the Central Alps, Switzerland. Tectonics 10, 599–620.

Sinclair, H.D. & Allen, P.A. 1992: Vertical versus horizontal motions in the Alpine orogenic wedge: stratigraphic response in the foreland basin. Basin Research 4, 215–232.

Sinclair, H.D. 1997: Flysch to Molasse transition in peripheral foreland basins: The role of the passive margin versus slab breakoff. Geology 25, 1123–1126.

Slingerland, R. & Smith, N.D. 1998: Necessary conditions for a meandering-river avulsion. Geology 26, 435–438.

Spiegel, C., Kuhlemann, J., Dunkl, I., Frisch, W., von Eynatten, H. & Kadosa, B. 2000: Erosion history of the Central Alps: Evidence from zircon fission track data of the foreland basin sediments. Terra Nova 12, 163–170.

Spiegel, C., Kuhlemann, J., Dunkl, I. & Frisch, W. 2001: Paleogeography and catchment evolution in a mobile orogenic belt: The Central Alps in Oligo-Miocene times. Tectonophysics 341, 33–47.

Spiegel, C., Siebel, W., Frisch, W. & Berner, Z. 2002: Sr and Nd isotope ratios and trace element geochemistry of detrital epidote as provenance indicators: implications for the reconstruction of the exhumation history of the Central Alps. Chemical Geology 189, 231–250.

Stolar, D., Roe, G.H. & Willett, S.D. 2006: Evolution of a critical orogen under various forcing scenarios: findings from a numerical sandbox. In: Willett, S.D., Hovius, N., Brandon, M. & Fisher, D.M. (Eds.): Tectonics, Climate, and Landscape Evolution. Geological Society of America Special Paper 398, 240–250.

Strunck, P. 2001: The Molasse of Western Switzerland. Unpublished PhD thesis, University of Bern, 146 pp.

Strunck, P. & Matter, A. 2002: Depositional evolution of the western Swiss Molasse. Eclogae Geologicae Helvetiae 95, 197–222.

Stürm, B. 1973: Die Rigi-Schüttung. Sedimentpetrographie, Sedimentologie, Paläogeographie, Tektonik. Unpublished PhD thesis, University of Zurich, 98 pp.

Von Rotz, R., Schlunegger, F., Heller, F. & Villa, I. 2005: Assessing the age of relief growth in the Andes of northern Chile; magneto-polarity chronologies from Neogene continental sections. Terra Nova 17, 462–471.

Willett, S.D. 1999: Orogeny and orography: The effects of erosion on the structure of mountain belts. Journal of Geophysical Research 104, 28957–28981.

Willett, S.D., Beaumont, C. & Fullsack, P. 1993: Mechanical model for the tectonics of doubly vergent compressional orogens. Geology 21, 371–374.

Willett, S.D., Schlunegger, F. & Picotti, V. 2006: Messinian climate change and erosional destruction of the central European Alps. Geology 34, 613–616.

Whipple, K.X. & Meade, B.J. 2004: Controls on the strength of coupling among climate, erosion, and deformation in two-sided, frictional orogenic wedges at steady state. Journal Of Geophysical Research-Earth Surface 109, doi:10.1029/2003JF000019.

Manuscript received February 1, 2007
Revision accepted March 10, 2007
Editorial handling: Hanspeter Funk, Helmut Weissert
Published Online First November 6, 2007